



# HHS Public Access

Author manuscript

*Med Phys.* Author manuscript; available in PMC 2018 June 01.

Published in final edited form as:

*Med Phys.* 2017 June ; 44(6): 2595–2612. doi:10.1002/mp.12227.

## Motion Management Strategies and Technical Issues Associated with Stereotactic Body Radiotherapy of Thoracic and Upper Abdominal Tumors: A Review from NRG Oncology

**Edward D. Brandner<sup>a</sup>,**

Department of Radiation Oncology, University of Pittsburgh Cancer Institute and UPMC CancerCenter, Pittsburgh, Pennsylvania 15232

**Indrin J. Chetty,**

Department of Radiation Oncology, Henry Ford Health System, Detroit, Michigan 48202

**Tawfik G. Giaddui,**

Sidney Kimmel Cancer Center, Sidney Kimmel Medical College, Thomas Jefferson University, Philadelphia, Pennsylvania 19107

**Ying Xiao,** and

Imaging and Radiation Oncology Core (IROC), University of Pennsylvania, Philadelphia, Pennsylvania 19104

**M. Saiful Huq**

Department of Radiation Oncology, University of Pittsburgh Cancer Institute and UPMC CancerCenter, Pittsburgh, Pennsylvania 15232

### Abstract

The efficacy of stereotactic body radiotherapy (SBRT) has been well demonstrated. However, it presents unique challenges for accurate planning and delivery especially in the lungs and upper abdomen where respiratory motion can be significantly confounding accurate targeting and avoidance of normal tissues. In this paper we review the current literature on SBRT for lung and upper abdominal tumors with particular emphasis on addressing respiratory motion and its affects. We provide recommendations on strategies to manage motion for different, patient specific situations. Some of the recommendations will potentially be adopted to guide clinical trial protocols.

### Keywords

stereotactic body radiotherapy; SBRT; lung; respiratory motion; abdomen; gating; 4D

---

<sup>a</sup>Author to whom correspondence should be addressed. Electronic mail: brandnere@upmc.edu, Department of Radiation Oncology, 5150 Centre Avenue, 5<sup>th</sup> Floor room 542, Pittsburgh, PA 15232.

### CONFLICT OF INTEREST DISCLOSURE

The authors have no relevant conflicts of interest to disclose.

## 1. INTRODUCTION

Advanced treatment techniques such as Intensity Modulated Radiation Therapy (IMRT) and Stereotactic body radiotherapy (SBRT) are capable of delivering highly conformal radiation doses. Furthermore, SBRT uses hypofractionation and high local doses to extra-cranial diseases such as peripheral stage I non-small cell lung cancer (NSCLC) and has been reported to provide excellent local control and survival comparable to surgery<sup>1-3</sup>. In order to spare critical structures and normal tissue, SBRT uses tight margins and accommodates inhomogeneous dose distributions. However, internal target motion may greatly affect the conformal radiation therapy for the management of thoracic and abdominal lesions<sup>4</sup>. Respiration is the most relevant source of motion for these lesions including lung, liver, and pancreatic cancer<sup>5</sup>. In particular, respiratory motion of lung tumors has been considered to be one of the largest sources of uncertainty in the radiotherapy of lung cancers<sup>6</sup>. Therefore, for the management of cancer in these patients, the respiration induced motion of lung and upper abdominal targets and critical structures must be monitored and accounted for.

Respiration induced motion may also lead to artifacts in images from computed tomography (CT), cone-beam computed tomography (CBCT), magnetic resonance imaging (MRI), and positron emission tomography (PET) because the typical image acquisition time per slice of 1 s or less is only a fraction of a respiratory cycle. Although any single slice appears unaffected by respiratory motion, consecutive slices occur at different phases of the respiratory cycle resulting in errors in the apparent size, shape, location, and volume of anatomic objects<sup>7-9</sup>. The effects on the image of the patient and on the dose distribution vary widely depending on a variety of factors such as the magnitude and frequency of the motion, the reproducibility of the motion during a single fraction (intrafraction), the reproducibility of the motion from day to day (interfraction), and the proximity of moving targets to organs at risk. Respiratory motion, if not taken into consideration, leads to artifacts and uncertainties in imaging and consequently affects the whole treatment process diminishing the accuracy of radiation therapy during imaging, planning, and treatment delivery<sup>10</sup>. Subsequently, these effects on planning and diagnostic images lead to uncertainties in localizing targets and critical structures, in addressing inhomogeneities, and in choosing planning margins. Target localization in image guided radiation therapy (IGRT) is also affected. Therefore, respiration induced motion must be addressed at all steps of the planning and treatment processes.

In this paper, we review the literature on respiratory motion as it pertains to SBRT including its measurement, reproducibility, monitoring, and management. Techniques including large treatment margins, respiration limiting devices, breath hold, gating, and tumor tracking are all evaluated.

This paper has also been reviewed by NRG Oncology who anticipates using it to help define guidelines for multi-institutional clinical trials involving SBRT for tumors of the thorax and upper abdomen. NRG Oncology is a non-profit research organization that conducts oncologic clinical research; broadly disseminates research results; and combines the work of the National Surgical Adjuvant Breast and Bowel Project (NSABP), the Radiation Therapy Oncology Group (RTOG), and the Gynecologic Oncology Group (GOG).

## 2. MOTION IN RADIATION THERAPY

### 2.A. Extent of Motion

Respiration is quasi periodic with a relatively predictable pattern for each patient<sup>11</sup>. Respiratory motion is patient specific<sup>12</sup>, and respiratory characteristics may vary in period, amplitude, and regularity<sup>13</sup>. Respiratory motion patterns can vary between fractions and even within a fraction<sup>14</sup>; therefore, there are no general patterns of respiratory behavior that can be assumed for a particular patient prior to observation<sup>15</sup>. Lung tumor motion was found to be associated with diaphragm motion, the superior-inferior tumor location in the lung, the size of the gross tumor volume (GTV), and the T stage of the disease<sup>16</sup>. The range of respiratory motion has been reported to be up to 50 mm<sup>15, 17–22</sup>. The largest tumor motions were observed in the lower lung<sup>13, 16</sup>. It was also observed to be largest in the superior-inferior direction with increasingly smaller components in the anterior-posterior and left-right directions<sup>15, 16, 23</sup>. However when generally considering lung tumors without respect to their locations within the lung, the tumor motion is typically less than 5 mm<sup>16</sup>. Liu et al reported that only about 40% of lung tumors move more than 5 mm and about 12% moved more than 10 mm<sup>16</sup>. However, organs in the upper abdomen such as the liver, kidneys, and spleen move significantly as a result of respiration—typically more than 10 mm<sup>23, 24</sup>.

### 2.B. Internal Target Volume (ITV)

Tumor motion must be quantified for treatment purposes<sup>23</sup>. The International Commission on Radiation Units and Measurements (ICRU) specified in its ICRU reports 50 and 62<sup>25, 26</sup> the different terminologies that are needed to define the target volume. In order to account for tumor motion, the ICRU introduced, in its ICRU report 62, the concept of an internal target volume (ITV). The ITV accounts for geometric uncertainties due to physiological organ motion which may include movement of the bowel, beating of the heart, or respiration. It also accounts for changes in tumor size and shape. ITV is defined as the clinical target volume (CTV) plus an additional margin to account for the aforementioned movement uncertainties and possible changes in tumor shape and size. The margin required is known as the internal margin (IM) and may be asymmetric based on the location within the body. To determine an ITV for a lung or upper abdominal tumor, the GTV is first delineated on each image representing the various respiratory bins that constitute the four-dimensional (4D) CT, PET, or MR imaging. The GTV is expanded to the CTV to account for microscopic disease. The ITV is then determined to be the envelope of motion of the CTV. The concept of the internal gross tumor volume (IGTV) was proposed as another method to more efficiently determine the ITV<sup>27</sup>. The IGTV expands the GTV to explicitly account for the GTV's variations in position, size, and shape which can be derived directly from imaging studies<sup>28</sup>. In this method, the ITV is determined to be the IGTV plus a margin that accounts for microscopic disease. A margin is then added to the ITV to account for patient setup uncertainties, and this new volume is the planning target volume (PTV). Figure 1 illustrates these volumes: the red contour is the GTV, the yellow is the IGTV, the green is the ITV, and the blue is the PTV.

Information on the extent of tumor motion is vital to assigning appropriate margins for radiotherapy<sup>9</sup>. Lung and upper abdominal tumor motion can be measured using different

techniques including: fluoroscopy<sup>13, 29</sup>, Cine MRI<sup>30</sup>, 4D MRI<sup>31, 32</sup>, slow CT<sup>33</sup>, breath hold CT<sup>34</sup>, 4D CT<sup>16, 35–37</sup>, 4D PET<sup>38–40</sup>, and ultrasound<sup>41, 42</sup>.

## 2.C. Imaging studies for motion measurement and evaluation

**2.C.1. Fluoroscopy**—The earliest method for observing and measuring motion particularly in lungs was fluoroscopy<sup>13, 23, 43</sup>. Fluoroscopy is limited in that it cannot provide cross-sectional anatomical information, and it depends on high contrast for visualization such as implanted fiducials or soft tissue in lungs<sup>13</sup>. It is relatively quick, and in conjunction with IGRT localization, it may be used to confirm tumor or organ motion at the time of treatment<sup>44</sup>.

**2.C.2. 4D CT**—4D CT or motion correlated CT is a powerful method for observing internal organ motion. A 4D CT data set includes multiple 3D images each of which represents a different portion or bin of the respiratory cycle. Generally, the binning methods used are either phase binning—associating each 3D CT image with a phase or fraction of the breathing cycle period—or amplitude binning—associating each 3D CT image with a fraction of the full breathing amplitude. Each 3D image in the 4D CT image set has a common phase or fraction of the amplitude.

A 4D CT is acquired either prospectively or retrospectively. In prospective respiration correlated CT, CT images are acquired only at one respiratory bin at a time. By repeating CT image acquisitions for the individual respiratory bins, each bin of respiration can have a corresponding 3D CT image. Retrospective respiration correlated CT is acquired in the following sequence:

1. at every table location, multiple axial CT images are acquired along the superior-inferior direction of the patient so that the entire respiratory cycle is represented;
2. simultaneously the respiration signal is acquired;
3. the respiration signal is synchronized with the CT images;
4. the acquired projection CT images are then post-processed according to the respiratory bin associated with each image resulting in multiple 3D CT image data sets each of which represents a specific breathing bin of the patient's respiratory cycle.

Often, the 4D CT image set includes 10 different 3D CTs. Irregular respiration makes the acquisition of high-quality 4D CT images very challenging<sup>45</sup>. The method of binning the CT images based on the respiratory signal can affect the quality of the 4D CT images. In phantom studies, Abdelnour et al found that “consistency error” (which they define as a measure of the ability to correctly bin over repeated cycles: average binning error  $\pm$  standard deviation within one bin) ranged from 11%  $\pm$  14% to 20%  $\pm$  24% for amplitude binning and from 18%  $\pm$  20% to 30%  $\pm$  35% for phase binning<sup>46</sup>. This suggests that amplitude binning more accurately bins the images, but it is more sensitive to irregular breathing particularly to amplitude irregularities which can cause image gaps<sup>46</sup>. Binning methods are an active area of research. One such study relies on Fourier transforms of the CT images and on internal anatomical structures to sort the 4D CT images<sup>47</sup>. The technique they employ does not rely

on external surrogates to track respiratory motion, and the results suggest that their method has fewer artifacts than a method that relies on external surrogates<sup>47</sup>.

**2.C.3. 4D CBCT imaging**—A cone beam computed tomography (CBCT) scanner integrated with a linear accelerator can be a powerful tool for motion evaluation of tumors and organs on the treatment table. Respiratory correlated CBCT has been developed and consists of retrospectively sorting images in projection space yielding subsets of projection images that each corresponds to a certain breathing phase. These subsets are then reconstructed to form a set of 4D CBCT images. Sonke et al also used the diaphragm position in the projections to sort the images instead of using an external surrogate to define the respiratory phase of each projection<sup>48</sup>. They found that the motion artifacts found in 3D CBCT images were substantially reduced by switching to 4D CBCT images; however, the quality of 4D CBCT images is adversely affected by breathing irregularities and aliasing artifacts caused by the limited number of projections for each breathing phase<sup>48</sup>. When comparing fluoroscopic images to the 4D CBCT images of a phantom simulating brathing, they found that the phantom's center of gravity differed by less than 1 mm<sup>(48)</sup>.

**2.C.4. 4D PET/CT imaging**—4D PET/CT scans can be used to add respiratory correlated functional imaging to a 4D CT scan. Following a 4D CT scan, a 4D PET scan is acquired in the gated mode. Based on a respiratory signal, the respiratory cycle is divided into phase bins of equal time and each PET signal is correlated with its respective phase. 4D PET/CT imaging has been shown to be a clinically feasible method to correct for respiratory motion artifacts in PET images including the reduction of smearing, improved accuracy of the PET to CT co-registration, and an increase in the measured SUV<sup>38–40</sup>

**2.C.5. 2D Cine MR imaging**—Cine MR images can be used to characterize tumor motion and to develop a gating scheme for radiotherapy particularly for abdominal cancer. In a study by Heerkens et al, 2 cine MRI scans of 60 s each were performed in 15 pancreatic cancer patients—1 in the sagittal direction and 1 in the coronal direction<sup>49</sup>. A Minimum Output Sum of Squared Error (MOSSE) adaptive correlation filter was used to quantify tumor motion in each orthogonal direction (craniocaudal, lateral, and anteroposterior). They examined the stability of the breathing phases and created a gating window assessment that incorporates tumor motion, treatment time, and motion margins. It was found that gated deliveries for radiotherapy of pancreatic cancer is best performed around the end exhale position and that motion patterns and motion amplitude differ substantially between individual patients<sup>49</sup>. Cine MRI images have been used to detect larger differences in hepatic intra-fraction tumor motion when compared with free breathing 4D CT images most notably in the superior/inferior direction<sup>50</sup>. Cine MRI images may be useful when treating without respiratory management particularly in patients with unreliable 4D CT imaging<sup>50</sup>. Among other factors, the absence of ionizing radiation using MRI has facilitated the application of cine MRI for the development of motion models in several different treatment sites including the abdomen<sup>51</sup>, thorax<sup>52, 53</sup>, liver<sup>50, 54</sup>, breast<sup>55</sup>, and rectum<sup>56</sup> among other sites. The emergence of on-line MRI-guided radiation delivery has also permitted the increased utilization of cine MRI techniques for real-time motion assessment and the construction of motion models<sup>57</sup>.

**2.C.6. 4D MR imaging**—4D MR images can also be used to image the motion of abdominal tumors and organs<sup>31</sup>. Hu et al used an external bellows to monitor respiration and to trigger image acquisitions at predetermined respiratory amplitudes<sup>31</sup>. The respiratory signal was also linked to each image so that it could be sorted into the appropriate respiratory phase resulting in a 3D MR image for each respiratory phase<sup>31</sup>. Cai et al compared 4D MR images with 2D cine images of a phantom and found the absolute agreement to be within 1 mm<sup>32</sup>. 4D MRI has been used to assess motion for several other treatment sites including the lung<sup>58</sup>, liver<sup>59</sup>, and abdomen<sup>51, 60</sup> among others.

**2.C.7. 4D Ultrasound**—4D ultrasound is a technology under development for 4D abdominal imaging and tracking<sup>41, 42</sup>. It might find a niche in the future. Table I lists advantages and disadvantages of the various imaging modalities.

## 2.D. Images for radiotherapy treatment planning

4D CT images are often used for target and critical structure delineations and may be supplemented with 4D PET/CT, Cine MRI, 4D MRI, fluoroscopy, and/or 3D CT images. From these images the GTV, IGTV, CTV, ITV, and PTV are defined. Because 4D image sets represent the GTV at various respiratory phases, a number of 3D images corresponding to the different respiratory phases must be evaluated together to identify the range of motion of the GTV (and/or critical structures) among the various phases and particularly the phases used for treatment delivery. The GTV or critical structures can be delineated on each image of the 4D image set. The individual contours can then be combined on one of the images in the set corresponding to a given phase. This given phase may be the end expiration phase or the phase nearest the midpoint of the breathing cycle (CT50 where CT0 is end inspiration) if treated with gating near end expiration, or it may be the mid-ventilation phase if treated with free breathing.

A Maximum Intensity Projection (MIP) image can be created from the image set; however, this is most appropriate in the lungs where the contrast is between the GTV and lung and where other structures will not obscure the GTV. The MIP image represents the highest intensity value encountered along the viewing ray for each pixel in the volumetric dataset for the respective breathing phase. The summation of MIP images for each breathing phase therefore results in a composite view of the lung tumor incorporating all phases of motion. An Average Intensity Projection (AIP) can be created from the image set and represents the average motion of the GTV (and critical structures) over the phases included. A study by Park et al found MIP images to be accurate to within 2–3 mm of the real target motion span for regular (constant amplitude and period) target motions but could underrepresent the motion span by more than 10 mm for irregular motion<sup>62</sup>. Tian et al compared 3D free breathing scans with MIP and AIP images by calculating the same plan to each scan while using the same target volume contours to evaluate the dosimetric effects caused by the different CT datasets<sup>61</sup>. They found slightly better target volume coverage using MIP images<sup>61</sup>. The free breathing scans were more prone to image artifacts<sup>61</sup>. If targets are close to denser tissue, the target and other tissues may overlap and obscure the target in the MIP images<sup>61</sup>.



## 2.E. Consistency of breathing

Measuring the effects of respiratory motion is necessary for planning, but it may not be sufficient for treatment delivery. Respiration can vary from moment to moment in amplitude and period; phase relationships from one anatomical location to another can vary; and baseline drifting can be observed<sup>37, 63, 64</sup>. Baseline drifts—a change in the mean position of a waveform measured over several periods (including the respiratory trace, the tumor, or an organ) are particularly problematic<sup>37, 64–67</sup>. These studies carefully evaluated variables in respiration. When evaluating respiratory motion, and the variables affecting it for each patient, the extent of uncertainty is critical to understand. For instance, a baseline drift of 2 mm is expected to be adequately compensated for by a 5 mm margin for motion<sup>68</sup>.

Although respiration is generally inconsistent, the end expiration phase is relatively stable and less affected by these inconsistencies. Furthermore, most people generally spend more time near end expiration than near any other phase<sup>13, 67, 69</sup>. Therefore, the end expiration phase or CT50 is often used for contouring, planning and evaluation. However, the lung volume is least at end expiration, so with everything else being equal, the percentage of lung receiving any given dose will be higher. In a dosimetric study planning SBRT for pancreatic cancer, Taniguchi et al found a reduction of dose to the duodenum using the end expiration phase as opposed to the end inspiration phase due to the changing anatomical relationship of the duodenum to the pancreatic tumor caused by respiration.<sup>70</sup> The V20 to the duodenum averaged 5.9cc when planned on end expiration and 7.2cc when planned on end inspiration<sup>70</sup>.

A simulation study by St. James et al illustrated the potential problem with relying on a motion study at one time to quantify motion at another time<sup>71</sup>. Their simulations suggested that the part of the planned ITV could be outside of the treated ITV more than half of the time for small target volumes when respiration is inconsistent, and this emphasizes the need for strategies that mitigate the problems with inconsistent respiration<sup>71</sup>. Ge et al compared 4D CT measurements of fiducials to fluoroscopic measurements to arrive at essentially the same conclusions as St. James et al<sup>72</sup>. Section 4.F.3 addresses the dosimetric effects of various CT datasets used for treatment planning. Section 3 discusses several strategies can be used to mitigate the effects of respiratory motion including the use of large margins, respiratory limiting devices, breath hold techniques, gating, and target tracking.

## 3. METHODS OF ADDRESSING MOTION

### 3.A. Large margins

The simplest and historically most common method for accommodating intrafraction motion is to use large margins that cover the full range of motion. As has already been noted, respiration-induced tumor motion is anisotropic; therefore, the internal margins should also be anisotropic<sup>27</sup>. These margins are best defined after measuring the motion of the target volumes and/or the critical structures. Although reported values of target or organ motion are valuable for reference, they should not be exclusively relied upon to choose treatment planning margins for SBRT or stereotactic radiosurgery (SRS).

Even though sufficiently large margins can cover the full range of motion of a target or avoid the full range of motion of an organ at risk, other issues remain. Large margins which are required to cover the tumor motion due to respiration may lead to unnecessary irradiation of normal tissues near the target. The effects of tumor motion need to be minimized to focus the prescribed dose on the target and decrease complication rates in normal tissues<sup>73</sup>. As discussed in section 4.A below, the MLC interplay effect might be significant, but large margins cannot limit these effects. Any significant change in respiration (i.e. coughs, sneezes, baseline drifts, etc.) might shift the target volume outside of the large treatment margins or shift critical structures inside of the treatment margins. In addition, such changes may not be observed and cannot be addressed unless breathing is monitored during the treatment.

### 3.B. Respiration limiting techniques/devices

Tumor or critical structure motion can be restricted through abdominal compression<sup>74–78</sup>. The application of abdominal pressure during imaging and treatment delivery is used by many centers to minimize respiration-induced tumor motion for both lung and liver lesions. Patients are forced to take shallow and fast breaths when their upper abdomens are pushed down by a pressure device to limit diaphragm caudal excursion. Heinzerling observed a significant difference in the control of both superior–inferior (SI) and overall motion of lower lobe lung and liver tumors with the application of medium and high compression when compared with no compression<sup>76</sup>. The mean overall tumor motion was 13.6 mm, 8.3 mm and 7.2 mm with no compression, medium compression, and high compression respectively<sup>76</sup>. Wunderink et al conducted a study on the effectiveness of different levels of abdominal compression on reducing respiration induced motion of liver tumors; their study included 12 patients<sup>78</sup>. They reported that the mean excursions were reduced to less than 5 mm in all directions for 10 of the 12 patients<sup>78</sup>. The two exceptions had cranio-caudal excursions reduced from 20.5 mm to 7.4 mm for one patient and from 21.1 mm to 5.9 mm for the other patient<sup>78</sup>. Eccles et al investigated the effectiveness of abdominal compression in reducing liver tumor motion using cine T2-weighted MRI images<sup>75</sup>. They reported a mean decrease in tumor motion with abdominal compression of 2.3 and 0.6 mm in the craniocaudal and anterior-posterior directions, respectively<sup>75</sup>. They concluded that a clinically significant (>3 mm) decrease in tumor motion was observed in 40% of patients and an increase in tumor motion was observed in <2% of patients in the craniocaudal direction<sup>75</sup>. Bouilhol conducted a study on twenty seven patients with non-small cell lung cancer<sup>74</sup>. All patients underwent two 4D CT scans with and without abdominal compression. They determined tumor motion amplitude, defined the ITV, and evaluated the influence of abdominal compression on lung dose-volume histograms. They observed that the most significant impact of abdominal compression was obtained in patients with lower lobe tumors<sup>74</sup>. Minor or negative effects of compression were observed on other patients and lung sparing was not substantially improved<sup>74</sup>. Mampuya et al compared the differences of overall survival (OS), local control (LC) and disease-free survival (DFS) in patients with non-small lung cancer treated with stereotactic body radiotherapy (SBRT) for primary lung cancer with and without abdominal compression<sup>77</sup>. They reported that the differences in the 3-year OS, LC, and DFS rate between the two groups were not statistically significant, and



they conclude that abdominal compression along with bony anatomy alignment provided no benefit to their patients<sup>77</sup>.

Active breathing control (ABC) is another method for decreasing respiration-induced tumor motion during a course of radiotherapy<sup>79–81</sup>. It is used to limit respiratory motion repeatedly and reproducibly for a period of time that can be comfortably tolerated by the patient. Breathing is temporarily suspended in a reproducible phase of the respiratory cycle. The operator of the device uses a computer-controlled valve to close the flow of air to the patient at a predetermined point in the respiratory cycle, causing a controlled breath hold. A nose clip is used to prevent nasal breathing and to ensure that patients breathe through the mouthpiece. The ABC system usually digitizes breathing volumes throughout the breathing cycle. In this way, visual control of the breathing cycle is possible. Both the inspiration and expiration paths of patients' airflow can be temporarily closed at a predetermined flow direction and breathing volume. The CT or radiotherapy treatment machine is activated only during the time when breathing is temporarily suspended. Wong et al reported that scan artifacts associated with normal breathing motion were not observed in the ABC scans and the liver volumes were reproducible at about 1%, and lung volumes were reproducible to within 6% in scans with ABC<sup>81</sup>. Dawson reported that no motion of the diaphragm or hepatic microcoils was observed on fluoroscopy during ABC breath holds<sup>79</sup>. Gagel reported a statistically significant reduction of respiratory motion in the upper, middle, and lower regions of the chest when ABC was used<sup>80</sup>. For thirty-six patients with unresectable tumors of the chest included in their study, the mean displacement ranged from 0.24 mm (chest wall/tracheal bifurcation) to 3.5 mm (diaphragm) for expiration and shallow breathing, and it ranged from 0.24 mm (chest wall) to 5.25 mm (diaphragm) for normal inspiration<sup>80</sup>.

### 3.C. Breath hold

Respiratory motion can be restricted via breath hold techniques. A highly reproducible breath hold CT scan can be acquired for treatment planning, and the breath hold can be repeated daily during radiation therapy. Various respiration monitoring tools are available to assist in maintaining the reproducibility of breath holds, and such tools are essential for accurate SBRT or SRS treatment using breath hold techniques. These monitors include spirometers<sup>82</sup>, cameras tracking reflective markers on the torso<sup>83, 84</sup>, camera or laser systems that directly track the torso (e.g. AlignRT® by VisionRT Ltd., London, UK and C-Rad Sentinel™ by C-RAD AB, Uppsala, Sweden)<sup>85, 86</sup>, mechanical devices tracking the torso<sup>87</sup>, strain gages affixed to the torso<sup>82</sup>, thermal sensors near nostrils<sup>82</sup>, fluoroscopic images of implanted fiducials<sup>88</sup>, and implanted transponders<sup>85</sup>.

Spirometers can be used to measure the volume of a breath and can be attached to valves to limit breath holds to specific volumes such as with ABC. Video coaching or audio-video coaching can be used to guide the patient to hold his/her breath at repeatable positions in a breathing phase. This is discussed below in Section 3.F.

Several factors must be considered when choosing the breathing phase and depth at which to have patients hold their breath. The end expiration phase is the most reproducible phase<sup>13, 66, 89, 90</sup>. Nakamura et al found a 5 mm internal margin was necessary to account for variations in GTV (pancreas) position with repeated, video-coached breath holds at end

expiration<sup>91</sup>. However, not all patients can tolerate repeatedly holding their breath especially at end expiration<sup>92</sup>. The end inspiration phase is not as reproducible as the end expiration phase, but lung volumes are largest at deep inspirations improving the lung DVH<sup>89</sup>.

Note that when acquiring planning CT's, breath hold volumes may differ from free breathing volumes even if the phases match<sup>93,94</sup>. It is imperative that the planning CT be acquired in the same manner as treatments will be performed.

### 3.D. Gating

Treatments can also be synchronized with the respiratory motion by gating the treatments using a breathing monitor. By setting thresholds within the breathing monitor, the beam can be turned on and off at specific breathing amplitudes or phases. Typically a 4D CT is acquired to determine which phases or amplitudes to include within the gating window. The window is chosen to limit the target and/or critical structure motion to acceptable limits (e.g. within 5 mm of end expiration)<sup>44, 85</sup>.

Much work has been done to evaluate the reproducibility of respiratory gating methods, and the evaluation is critically dependent on the method of monitoring respiration, on the choice of whether or not to coach the patient, and on how coaching is implemented. The most accurate method of monitoring the target location is to directly observe it; however, this is often not possible. Fiducials can be placed in the target and monitored by using fluoroscopy, kV imaging, or, if the fiducial is a transponder, by using technology designed for the transponder<sup>85</sup>. Shirato et al developed a fluoroscopic real-time tumor tracking technique consisting of four sets of diagnostic X-ray sources and imagers (any two of which offer an unobstructed view of the patient however the gantry is rotated) which are connected to an image processor, a display, and a gating control unit<sup>88</sup>. They used the system to gate the linac when the position of a moving gold marker (the system recognizes the marker 30 times per second using any two X-ray systems) is at its planned target position within a given tolerance. They tested the accuracy of the system to be within 1.5 mm and measured the additional dose from the diagnostic x-rays in a phantom to be from 0.01% to 1% of the target dose for a 2.0-Gy irradiation of a chest phantom<sup>88</sup>. The geometric performance was also evaluated in 4 patients with lung cancer. The range of motion of the tumor markers during irradiation was 2.5–5.3 mm but would have been 9.6–38.4 mm without tracking<sup>95</sup>.

Implanting fiducials is invasive and involves certain risks (e.g. possible pneumothorax)<sup>85</sup>. Other techniques do not directly monitor the target but monitor respiration. This indirect monitor can be a marker on the chest or abdomen of the patient. It can be the displacement of the chest or abdomen itself. It can be a thermistor, a spirometer, or a strain gauge. Reproducibility of various techniques is discussed below in the section on coaching.

Several issues must be considered when choosing to gate radiotherapy. Gating will be based on either amplitude or phase. Phase-based gating is easier to coach, but the most recent studies suggest that amplitude-based gating has less residual motion<sup>66, 89, 96</sup>. As was already noted in an imaging study, Abdelnour et al found that amplitude-based binning was more consistent and accurate than phase-based binning<sup>46</sup>. In a study of 24 patients, George et al found the average residual motion to be up to 0.7 mm less for amplitude-based gating as

opposed to phase-based gating<sup>66</sup>. Gating is done around certain respiratory phases referred to as the treatment phases that are either around end inspiration or around end expiration. End expiration is more reproducible, but at end inspiration, the volume of lung receiving high doses of radiation is reduced<sup>89</sup>. Coaching is an important aspect of gated therapy and is discussed in the section on coaching (Section 3.F.). When using only a few respiratory phases for planning and for creating reference images, a CBCT acquired for patient alignment will have to be registered with the reference CT such that the treatment phases are properly aligned (e.g. if the reference CT represents the end expiration phase(s), the superior edges of the target volume in the CBCT should be registered with the reference CT)<sup>85, 97</sup>. 4D CBCT or fluoroscopic images can also be used to register daily alignment images with the reference images<sup>85, 97</sup>.

### 3.E. Tumor Tracking

Real-time dynamic multi leaf collimator (DMLC) tumor-tracking radiation delivery uses the DMLC to continuously align and reshape the treatment machine apertures to follow the target motion in real time. This allows for tighter margins to be applied and for adapting the dose delivery to the target motion<sup>98</sup>. Keall et al have used real time 3D DMLC tumor tracking with Volumetric Modulated Arc Therapy (VMAT)<sup>99, 100</sup>. The tumor position was measured electromagnetically, and new leaf positions were created to conform to the shape and location of the moving target at each instant. They reported a significant improvement in dose distribution to moving targets with DMLC tracking as compared with those without tracking<sup>99, 100</sup>. Falk et al also used real time DMLC tracking to adjust the MLC positions according to the target movement using the information from Varian's real-time positioning monitoring (RPM<sup>TM</sup>) system<sup>101</sup>. Plan validations with DMLC tracking gave much higher gamma index pass rates (98%) versus those with no motion compensation (70–75%)<sup>101</sup>. Davies et al experimentally validated an algorithm for DMLC tracking of a moving target during VMAT to investigate the potential of the Agility<sup>TM</sup> (Elekta AB, Stockholm, Sweden) multileaf-collimator for use in motion-compensated VMAT delivery<sup>102</sup>. They validated plans for five patients and reported an increase in the mean gamma index pass rate from approximately 60% without tracking to 88–93% with tracking in VMAT delivery<sup>102</sup>.

Tacke et al implemented specialized algorithms which continuously optimized and corrected the MLC aperture according to the motion of the target volume during the dose delivery<sup>103</sup>. This dynamic target tracking control system was designed for a Siemens 160 MLC. They experimented with various motion patterns on phantoms equipped with radiochromic films placed between solid water slabs and on a moving lung phantom. They reported an increase in the gamma success rate of validated plans from 19% to 77%<sup>103</sup>. The system's 400 ms latency and 5 mm leaf width limited its dosimetric accuracy<sup>103</sup>.

The Vero<sup>TM</sup> SBRT system uses a gimbaled linac to track tumors<sup>104</sup>. The beam is rotated around the linac assembly's center of gravity to track an implanted fiducial. Real-time beam positions recorded with an electronic portal imager, gimbal log files, and orthogonal X-ray images are acquired simultaneously, logged, and used to identify and track the fiducial<sup>104</sup>. Poels et al verified this technique on a phantom using tracking data from a liver patient and two lung cancer patients<sup>104</sup>. Their results indicated that gimbaled tracking could achieve a

90th percentile error of less than 3.5 mm based on electronic portal images and X-ray images<sup>104</sup>. Depuydt et al also reported on initial assessment of the Vero™ Dynamic Tracking workflow and concluded that the Vero™ tracking solution proved to be fully functional with performance comparable to other real-time tracking systems<sup>105</sup>.

The Synchrony™ Respiratory Tracking System (Accuray Oncology, Sunnyvale, CA) correlates external markers with orthogonal stereoscopic images of fiducials implanted in or near the target volume to create a model of the target motion<sup>63, 85</sup>. The model is then used to move the CyberKnife® robotic linear accelerator to track the target, and periodically additional X-ray images are acquired to verify and/or update the target motion model<sup>85, 106</sup>.

### 3.F. Coaching

Monitoring and evaluating respiration is essential to determining its effects on tumor and/or critical structure motion. Free-breathing is not consistent in period or amplitude; this makes predicting respiratory motion challenging and limits the usefulness of breathing evaluations<sup>63</sup>. As discussed in Section 3.D., implanted fiducials can be used to track tumor and/or critical structure motion; however, such invasive procedures have inherent risks and cannot always be used<sup>85</sup>. A technique that improves breathing reproducibility would improve the monitoring and evaluation of respiration. Using external surrogates to monitor breathing avoids the risks inherent to implanting fiducials. Coaching while monitoring the abdominal wall, chest wall, or lung tidal volume has been demonstrated to improve the reproducibility of respiration<sup>66, 87, 90, 107–111</sup>.

Ionascu et al found that external surrogates placed on the abdomen of each patient could localize the internal targets to within 5 mm<sup>112</sup>. Likewise, Koch et al found that the mid-upper abdominal wall movement was well correlated (correlation coefficient > 0.7) with the superior-inferior motion of internal structures for all patients imaged<sup>113</sup>. However, they found that anterior-posterior motion was not always well correlated<sup>113</sup>. Ahn et al measured an average correlation of 0.77 between internal organ positions (e.g. diaphragm) and skin markers using fluoroscopy studies<sup>73</sup>. However, Hoisak et al found that the abdominal wall displacement did not necessarily correlate well with tumor motion, and the correlation varied significantly even over different acquisitions during the same session for some patients (0.39–0.71 in one case)<sup>114</sup>. They found that the correlation between respiratory lung volume and tumor position was better but still not always satisfactory (0.51–0.77 in one case)<sup>114</sup>. None of these studies included coaching.

It is imperative that the techniques used to monitor and evaluate the motion also be used to monitor and treat the patient. Hunjan et al found that external marker motion was poorly correlated with the internal target motion when comparing end inspiration and end expiration breath holds with the same respiration phases under free breathing conditions<sup>94</sup>. Similarly, Haasbeek et al observed shifts of more than 5 mm at end inspiration and end expiration when comparing coached and uncoached 4D CT scans<sup>115</sup>.

With the introduction of audio coaching, the correlation between the abdominal wall position and the target position increased from a range of 0.89–0.97 to a range of 0.93–0.99 in Nakamura et al's study<sup>109</sup>. The correlations in Michalsky et al's study (17 of 21 cases had

Pearson correlation coefficients  $> 0.7$ ) and in Goossen et al's study (0.72–0.98) did not show as high a range as those in Nakamura et al's study (0.93–0.99), but they were still better than the uncoached correlations in Hoisak et al's study (0.39–0.71)<sup>90, 110, 114</sup>. Mageras et al also concluded that audio coaching improves breathing regularity<sup>111</sup>. However, audio coaching does tend to cause other changes in respiration. George et al and Nakamura et al noted that patients breath more deeply when following audio coaching<sup>66, 109</sup>.

Onishi et al introduced a video coach to improve the reproducibility of end inspiration breath hold positions<sup>87</sup>. With video coaching, the superior-inferior position reproducibility of an internal lung structure was found to be 2.0 mm on average, and without the coach it was 4.2 mm on average<sup>87</sup>.

Using audio/video coaching, Goossen et al found correlations ranging from 0.91–0.99<sup>90</sup>. Stock et al found the reproducibility of the marker position to improve from 0.745 without coaching to 0.930 with audio/video coaching at deep inspiration breath hold<sup>65</sup>. Kim et al found that the root mean square error of the diaphragm displacement was reduced from 2.6 mm to 1.6 mm with the introduction of audio/video coaching<sup>108</sup>. Likewise, the root mean square error of the period was reduced from 1.7 s to 0.3 s, and that of the baseline drift was reduced from 1.6 mm/min to 0.9 mm/min<sup>108</sup>. Neicu et al and George et al also demonstrated that breathing patterns are improved using audio/video coaching<sup>66, 107</sup>. Audio/video coaching improves the reproducibility of the target position and the correlation between it and surrogates; however, not all patients can follow audio/video coaching<sup>90, 107, 108</sup> or even just video coaching<sup>87</sup>.

## 4. TREATMENT PLANNING AND PHYSICS

### 4.A. Multileaf collimators (MLC) and respiration interplay

Because targets and critical structures can move significantly during treatments that involve MLC motion, these interplay effects must be considered. This was considered in TG-76 of the American Association of Physicists in Medicine (AAPM)<sup>93</sup>. The authors concluded that the large number of fractions in conventionally fractionated treatments “smooths out” the interplay effect resulting in satisfactory dosimetry as long as the full range of motion of the target was included in all of the treatment ports<sup>93, 116, 117</sup>. However, in SBRT the fractions are fewer in number and the modulation of the dose is higher; therefore, SBRT plans are expected to be more sensitive to the interplay effect<sup>68, 117–119</sup>. Stambaugh et al divided the effects of tumor motion on dose into two effects: gradient and interplay<sup>119</sup>. Gradient effects are caused by the tumor moving beyond the planned margins and outside of the high dose region, and interplay effects are caused by the tumor moving relative to the modulation of the dose which can be highly inhomogeneous in SBRT treatments<sup>119</sup>. Siochi et al<sup>68</sup>, Zhao et al<sup>120</sup>, and Chen et al<sup>118</sup> have shown that gradient effects are detrimental to SBRT treatments especially because PTV margins are so small in SBRT plans<sup>68, 118, 120</sup>. Stambaugh et al studied the MLC interplay effects with simulated motion up to 30 mm for typical SBRT plans, and found that the  $D_{\text{mean}}$  to the target did not decrease by more than 1% for typical breathing cycles<sup>119</sup>. Chen et al measured the interplay effects on an artificially highly modulated plan and found differences at the top of the sharp peaks of 12% for 10 mm of motion, 6% for 8 mm of motion, and 3% for 6 mm of motion<sup>118</sup>. Jiang et al evaluated the

dose to a single point in a moving phantom (20 mm of motion) and found that the interplay effect caused a maximum dose deviation of up to 18% for a single fraction (5 fields) and up to 30% for a single field<sup>117</sup>. The significance of the interplay effect increases as the amplitude of the motion increases, as the treatment fractions decrease, as the dose rate increases, and as the dose inhomogeneity increases making it a particular concern for lung and abdominal SBRT. Methods such as gating, abdominal compression, breath-hold, and tumor tracking can be used to limit motion during treatment and thus mitigate the interplay effect.

#### 4.B. General Considerations

Accurate treatment planning for the treatment of lung cancer is confounded by several technical factors including tissue heterogeneity and the physics of radiation transport in low density lung tissue, the impact of motion on dose distributions, technical issues related to treatment planning using 4D-CT datasets, and the physics of small field dosimetry which is of particular concern for the treatment of small lesions commonly encountered in SBRT. Sections 4.B-4.F will focus on a review of the literature and provide recommendations (where supported by data) pertinent to accurate treatment planning for cancer in the lung or upper abdomen. Comprehensive reviews of current techniques for lung cancer treatment planning and delivery are presented by Martel<sup>121</sup>, Senan et al<sup>122</sup>, and Slotman et al<sup>123</sup>. Comprehensive reviews of current planning and delivery techniques for cancers in the upper abdomen are presented by Davis et al<sup>124</sup>, Scorsetti et al<sup>125</sup>, and Solberg et al<sup>126</sup>.

The goal of treatment planning is to optimize the therapeutic ratio, that is, to maximize the dose to the target while minimizing dose to surrounding normal organs. This is challenging for lung and upper abdominal tumors given the often substantial respiration-induced motion and the factors listed above.

#### 4.C. Planning Margins

Motion management at the time of simulation is often handled using 4D-CT in which a motion envelope of the target can be generated. The motion envelope is referred to as the internal target volume (ITV)<sup>26</sup> and it accounts for respiration-induced movement of the clinical target volume (CTV) during treatment. The ICRU Report No. 62<sup>26</sup> also recommends that a margin (planning organ at risk volume, PRV) be added to an organ-at-risk to account for variation in the OAR position. Margins added to the ITV to create the PTV must be designed with an understanding of the random and systematic setup uncertainties associated with patient setup<sup>127</sup>. Imaging frequency has an impact on margins. In general, more frequent imaging (e.g. daily vs. weekly) allows one to better account for systematic and random uncertainties facilitating margin reduction<sup>128</sup>. Daily IGRT based setup has been shown to significantly reduce residual uncertainties and consequently planning margins<sup>129, 130</sup>.

For ITV-based treatment planning, in the context of locally advanced stage NSCLC, typical margins for the PTV are on the order of 5–10 mm if daily IGRT is employed during treatment. In the absence of motion compensation or daily IGRT, margins should be much larger (10–20 mm) to minimize the likelihood of missing the target<sup>131, 132</sup>. In the case of



SBRT, where motion management and daily IGRT are the recommended standard-of-care<sup>131</sup>, PTV margins can range from 3–10 mm<sup>123, 129, 133, 134</sup>. Margins tend to be larger in the superior-inferior direction where respiration-induced motion is more dominant relative to motion in the axial plane<sup>135</sup>. When gating is used for treatment, margins can generally be reduced and some groups have thus defined the PTV as CTV + 5 mm<sup>120, 136, 137</sup>. A margin expansion of a few millimeters is necessary to account for residual tumor motion and setup uncertainty<sup>120, 137</sup>. In a retrospective study using recorded tumor motion data, Zhao et al calculated the dose delivered to the PTV and CTV using the initial plan for 6 patients<sup>137</sup>. They found that a margin of 5 mm around the CTV for respiratory motion (baseline drifts) was sufficient to maintain 99% of the prescribed mean dose to the CTV<sup>137</sup>. Nelson et al acquired multiple (up to 8) 4DCT scans on each of 7 patients and analyzed the margin necessary to accommodate the GTV and CTV motion<sup>138</sup>. They found that the margin could be reduced up to 3 mm if the plans were gated using a 30% duty cycle; however, only 1 of their patients had respiratory motion greater than 10 mm<sup>138</sup>.

Importantly, gating margins must be designed with careful consideration of the strength of the surrogate used to assess the actual tumor position during treatment<sup>139</sup>. Studies have shown that with the use of external surrogates to track tumor motion, phase offsets exist, and the motion traces can sometimes be entirely asynchronous<sup>63</sup>. It has therefore been recommended, when external surrogates are used for evaluating the tumor position, that imaging be performed, at the very least prior to treatment, to assess the 3-D tumor motion trajectory<sup>63</sup> (e.g. fluoroscopy or 4D CBCT).

#### 4.D. Block Margins

In general, treatment plans should be designed to minimize dose to surrounding normal organs and thereby limit the risk of treatment toxicity. This implies that sharp gradients will exist in the dose fall-off outside of the target<sup>131</sup>.

3D-CRT planning must be performed with consideration of the “block” margin (PTV-to-MLC margin). For SBRT planning, RTOG/NRG protocols require the external border of the PTV to be covered by a much lower isodose surface than usually used in conventional radiotherapy planning—typically ~80% but ranging from 60–90% of the dose maximum<sup>140, 141</sup>. This implies highly heterogeneous dose distributions with hot spots within the GTV of 25% on average and ranging up to 67%<sup>140</sup>. The >90% 2-year local control rates associated with SBRT of early stage lung tumors may indeed be linked to these heterogeneous dose distributions. In order to generate such non-uniform dose distributions, the block margin should be small. Planning studies have shown that block margins of 0 mm for 3D-CRT plans yield optimal hot spots within the tumor while simultaneously forcing a much sharper dose falloff in the normal lung tissue. The sharper falloff results from steeper dose gradients when normalizing to a much lower isodose surface (60–90%) for the target<sup>142</sup>.

#### 4.E. Tissue Heterogeneity and Motion

In general, when electrons impinge upon low-density, lung-type tissue, they undergo significant lateral scattering causing energy to be transported away from the central axis.

This results in reduced central axis dose to the tumor and smearing of the edges of the dose profile<sup>143</sup>. When coupled with tumor motion (which tends to smear out dose distributions) the reduction in the tumor dose and in the coverage of the extent of the tumor can be significant. When dealing with small tumors, as in the case of SBRT, this problem is further confounded by the loss of lateral charged-particle equilibrium which results from the use of small field sizes. For small field conditions, the lateral ranges of the secondary electrons become comparable to (or greater than) the field size<sup>144</sup>. Under such circumstances, the dose to the target is determined primarily by the secondary electron interactions. Moreover, as the energy of the beam increases, the range of the secondary electrons increases causing increased lateral scattering into distal lung tissue and increasing the region of dose “re-buildup” in the tumor. Consequently, the dose reduction to the tumor is greater at higher energies<sup>145</sup>. Pencil beam (equivalent path-length type) dose algorithms do not account explicitly for transport of secondary electrons, and can therefore be severely limited in accuracy under non-equilibrium conditions. The AAPM Task Group No. 105<sup>143</sup> provides examples of numerous studies reported on the inaccuracies associated with pencil-beam type algorithms for dose calculations in the lung. The AAPM TG Report No. 101<sup>131</sup> recommends that pencil-beam algorithms not be utilized for SBRT-based lung dose calculations and that convolution-superposition or Monte-Carlo type algorithms be used to compute more accurate dose distributions.

Although convolution/superposition or Monte-Carlo-type algorithms are now available in most commercial treatment planning systems, beamlet calculations for IMRT optimization are often still computed using pencil-beam algorithms. This issue can be mitigated by performing an intermediate dose calculation using the convolution/superposition algorithm which is now currently available in some treatment planning systems. This problem can also be handled by performing Monte-Carlo-based beamlet calculations within the optimization routine<sup>146</sup>. With regard to management of motion in the IMRT setting, investigators have developed optimization approaches in which setup uncertainties or tumor motion are incorporated *a priori* into the optimization process to produce treatment plans that are robust to the motion<sup>147, 148</sup>. In particular, the Monte-Carlo-based fluence-translation method can be applied to account for systematic lung tumor motion especially in cases where the tumor trajectory can be estimated<sup>149</sup>.

#### **4.F. Other technical issues related to treatment planning of cancer in the lung or upper abdomen that involves motion**

Detailed studies involving large patient cohorts and capturing the issues associated with differences of lung tumors according to tumor location, size, differences in planning phase(s), and type of treatment (e.g. incorporating the full range of motion vs. gating or tracking) are quite limited. With the now standard-of-care use of 4D-CT for lung cancer treatment planning, the literature is scant with regard to information on the following pertinent topics. This section will summarize highlights relevant to the specific topics.

**4.F.1. What is the role of MIP in generating the ITV?**—Automatic tools have been developed to improve efficiency in the contouring of GTVs on multiple datasets to form an IGTV and the ITV. Studies have shown the MIP to be an effective tool for automatic

contouring of targets on multiple phases of the 4D-CT<sup>150–153</sup> but caution that the MIP should be validated against the ITV formed by contours on each of the respiratory-correlated CT datasets<sup>152</sup>. Other studies point out that the MIP cannot be used for tumors located in the mediastinum or for tumors located near normal tissues with equal or greater density (e.g. those near the diaphragm or in the upper abdomen)<sup>151</sup>.

#### **4.F.2. How many respiratory-correlated CT phases should be used to create the ITV?**

—Increasing the number of datasets in defining the ITV—while likely improving the accuracy of the ITV contour—increases the contouring workload significantly and thereby decreases clinical efficiency. Research on the topic of the optimal number of datasets is limited. In one study, investigators performed an analysis of 4D-CT datasets from 10 lung cancer patients focusing on the N phases closest to the exhale phase where N=6, 7, 8, 10<sup>154</sup>. In evaluating D95 of a given N relative to a plan based on N=10, some reduction (8/10 phases) was possible for most, but not all, of the patients, and the ITV reduction was small. They concluded that a general rule based on the number of datasets could not be established in creating the ITV<sup>154</sup>. In comparing N=2, 4, 10 phases for 15 lung patients treated without gating, other investigators found no statistically significant differences between N=4 (end-exhale/inhale and mid-exhale/inhale) and N=10 suggesting that the use of 4 phases is an efficient alternative to 10 phases in generating the ITV<sup>155</sup>. This study was previously corroborated by phantom experiments from an independent group<sup>156</sup>. In a study of patients treated for pancreatic cancer by Tai et al, they found that an ITV created using just 3 phases (end inspiration, end expiration, and the mid-exhale) overlapped with the ITV created with 10 phases with an accuracy of more than 95% if the target motion is 8 mm or less<sup>157</sup>. More comprehensive studies on the optimal number of datasets for generating the ITV for a large number of datasets with diverse tumor motion including hysteresis<sup>13</sup>, location, size, and/or other characteristics are clearly warranted.

Various tools have become available to assist with contouring including deformable registration and automatic segmentation. These tools can be valuable when propagating contours from phase to phase; however, they require careful validation and case-by-case evaluation.

#### **4.F.3. What is the most accurate CT phase for treatment planning?**

—In general, studies performed to determine possible dosimetric advantages among the free breathing (FB), MIP, and AIP, CT datasets are limited. In one particular study for 20 lung cancer patients being treated with SBRT, the authors concluded that dosimetric characteristics of AIP plans are similar to those of FB plans<sup>61</sup>. They also noted that FB datasets were more prone to significant image artifacts compared to AIP datasets, and because MIP datasets tend to overestimate or underestimate the target volume when the target is close to more dense tissues, the AIP dataset is most favored for planning and dose calculation for lung SBRT<sup>61</sup>.

Research on the time-weighted average tumor position in the 4D-CT dataset has shown that the mid-ventilation CT is able to accurately accommodate motion with a significant reduction in PTV margin compared to the standard free-breathing CT approach<sup>158</sup>. The AIP CT dataset, has also been shown to be a good surrogate for accurate lung cancer planning using 4D-CT<sup>159–161</sup>. In one such study, insignificant dose differences were noted between

the AIP CT and the full 4D-CT calculation (incorporating deformable image registration and dose accumulation) in both phantom experiments as well as patient-specific treatment plans justifying the claim that the use of the AIP CT enables simplification of the 4D dose calculations for lungs in clinical practice<sup>161</sup>.

In the context of gating, studies have shown that deep-inspiration breath-hold offers the potential to not only reduce respiratory motion but also increase normal tissue sparing from the increased lung volume<sup>162</sup>. However, the reproducibility of the deep-inspiration position must be carefully assessed, and the general applicability of this technique for lung cancer patients who often have significant co-morbidities (e.g. COPD) must be considered. Breath-hold approaches include the ABC device where the lung volume is controlled and patients with tumors in the thorax or abdomen are treated with breath-hold near end inspiration<sup>81</sup>. ABC enables margin reduction and normal tissue sparing; however, the applicability to the general lung cancer population must be considered given the often considerable co-morbidities among these patients.

**4.F.4. Are ITV or PTV density overrides necessary for accurate treatment planning?**—In forming the ITV, automatic tools such as the MIP are often utilized to improve efficiency. When the ITV from the MIP is mapped onto the planning CT (either a free-breathing CT or average CT) the anatomy between the MIP and planning CT is not necessarily aligned. This raises a concern about the surrounding anatomy of the target within the planning CT dataset. If one were to map the ITV contour onto a free-breathing CT with artifacts in the vicinity of the tumor, it is likely that the density of the tumor will not be uniform, i.e. the tumor might be fragmented and include parts of surrounding lung tissue. This scenario would create a possible problem with regard to dose coverage and/or optimization in the context of IMRT. The target is likely to receive inadequate dose coverage if it is comprised of significant low-density lung tissue. Under such circumstances, it is not unreasonable to consider overriding the target density in the planning CT dataset.

In one study, researchers compared VMAT plans created on free breathing scans (FBP), time averaged scans (AVGP), free breathing (FB) scans with the internal target volume overridden to tumor density (ITVP), free breathing scans with the PTV overridden to tumor density (PTVP), and FB scans using a hybrid scheme, in which the ITV was set to tumor density and the PTV minus the ITV was set to a density intermediate between lung and tumor (hybrid density, HP). The plans were created for phantom experiments and 5 patient-specific cases<sup>163</sup>. The authors concluded, based on the phantom measurements, that the hybrid density method (HP) may provide more accurate dose modeling and decreased normal lung irradiation for lung SBRT compared to the commonly used FBP and AVG planning approaches (for 3D plan using 1%/1mm gamma evaluation, HP passing rate = 85%, FBP passing rate = 69%, and AVG passing rate = 65%, but using 2%/2mm, all methods passed with greater than a 96% passing rate)<sup>163</sup>. For the patient cases, all methods yielded similar D95 values; however, the PTVP and HP plans yielded significantly lower conformity indices than the other techniques (e.g. 1.11 versus 1.13)<sup>163</sup>. In general, research on this specific topic is limited, and additional studies are necessary.

#### 4.G. Imaging for position verification and localization

Image guidance is imperative to achieve the accuracy in patient positioning and in target and normal tissue localization necessary for the tight margins required for SBRT<sup>164</sup>. Purdie et al found a mean difference of 6.8 mm when comparing bony anatomy alignment versus target alignment using CBCT. Their mean residual error after CBCT localization was 1.9 mm<sup>165</sup>. If fiducials are implanted in the target, planar images can localize the target, CBCT consistently localizes targets more accurately and provides necessary information regarding possible deformation and nearby organs at risk<sup>164</sup>. Higgins et al evaluated various interfraction imaging protocols to determine if daily CBCT imaging is necessary. They derived setup margins of 3–4 mm if daily CBCT was used versus 5–9 mm if CBCT was done less often than every fraction<sup>166</sup>.

Once localized, the target must remain localized for the duration of treatment which is more challenging for the long treatment sessions involved in SBRT. Hugo et al compared pretreatment CBCTs to post treatment CBCTs and calculated the 95% confidence level for the lung target shifts to be 2.4 mm superior-inferior, 2.3 mm anterior-posterior, and 1.9 mm left-right<sup>167</sup>. In a similar study, Purdie et al plotted the lung target shift versus the time between the initial CBCT and the repeat CBCT. They found that beyond 34 minutes, the shift grew larger with a mean deviation of 5.3 mm<sup>165</sup>.

Although a powerful tool for IGRT, CBCT is susceptible to artifacts due to respiratory motion<sup>48</sup>. Fluoroscopy is useful for evaluating motion<sup>44</sup>, but it does not provide volumetric information. 4D CBCT has been used on patients by Sonke et al. Over the treatment session, their mean deviation of 4.1 mm is slightly better than that in Purdie et al's study, but the time between imaging was 28 minutes as opposed to Purdie et al's average of 34 minutes<sup>132, 165</sup>. Sonke et al also evaluated the systematic and random localization inaccuracies in each direction: systematic inaccuracies of 0.8 mm left-right, 0.8 mm superior-inferior, and 0.9 mm anterior-posterior, random inaccuracies of 1.1 mm left-right, 1.1 mm superior-inferior, and 1.4 mm anterior-posterior<sup>132</sup>.

CBCT localization also lends itself to the possibility of adaptive planning. Various investigators have begun exploring the possibilities and challenges of adaptive planning as summarized by Mageras et al<sup>164</sup>.

CT-on-rails is another powerful tool for position verification and daily localization that also lends itself to adaptive planning. CT-on-rails integrates a diagnostic CT scanner into a radiotherapy treatment room. The distinguishing feature of such a system is the moving gantry CT scanner which is mounted on rails at the end of the treatment couch opposite the treatment gantry. The couch is usually rotated to 180° to acquire the daily image with the patient in the immobilization position. The couch is then rotated back to the linac side to proceed with treatment.<sup>168</sup> The in room CT image can be aligned with the reference CT (planning CT) based on soft tissue and bony contrast<sup>168, 169</sup>. CT-on-rails has the advantage of more consistent and accurate registration with the planning CT as compared with CBCT<sup>168</sup>, and it allows image guided adaptive radiotherapy by modifying the treatment parameters according to changes in the patient's anatomy before each treatment or during the course of radiotherapy<sup>169</sup>.

4D CT-on-rails was used for target localization for 10 free breathing liver SBRT patients and more accurately localized target volumes than 3D CBCT<sup>170</sup>. In another study, CT-on-rails was used along with on line adaptive planning for 10 pancreatic patients<sup>171</sup>. All daily CTs were acquired with gating and were registered with the planning CT (50% phase) with the center of mass of the ITV aligned<sup>171</sup>. Online adaptive planning based on the CT of the day effectively accounted for interfractional variations that cannot be corrected for by IGRT repositioning, and this offered improved OAR sparing and permitted smaller PTV margins<sup>171</sup>. Table I lists advantages and disadvantages of the various imaging modalities.

## 5. DISCUSSION AND CONCLUSION

The efficacy of SBRT for lung and upper abdominal tumors has been demonstrated. Accurate target coverage and protection of critical structures are paramount to effective SBRT, but motion poses a particular challenge for these sites. Based on this review of literature, several recommendations follow:

1. A motion study should be performed for all SBRT lung and upper abdominal tumors and critical structures using 4D CT, 4D PET/CT, Cine MRI, 4D MRI, and/or 4D CBCT techniques.
2. The full range of motion of the treatment phases for the target and nearby critical structures must be incorporated into planning contours.
3. Planning image data sets can be derived from MIP, AIP, end expiration, CT50, or free breathing CT images with the following caveats:
  - a. MIP and AIP images can be used for lung targets, but not abdominal targets.
  - b. MIP images can be used if the full range of motion of the target does not overlap the full range of motion of any other structure other than low density lung.
  - c. Free breathing CT images can be used if the phase of the free breathing CT matches a treatment phase.
  - d. When treating with gating near end expiration, the end expiration phase or the phase nearest the midpoint of the breathing cycle (CT50 where CT0 is end inspiration) can be used for lung or upper abdominal targets, or when treating with free breathing, the mid-ventilation phase can be used for lung or upper abdominal targets.
4. PTV margins must account for setup error, anatomic changes, and intrafraction movement of the target
  - a. Setup error should be measured or otherwise determined for every clinical situation. Typical setup error is 2–4mm with daily CBCT, but is usually larger without daily volumetric imaging.
  - b. Intrafraction movement increases with treatment duration particularly if the duration exceeds 30min.



- i. Larger PTV margins can be used to account for this movement.
    - ii. Reimaging during treatment can be used to mitigate this effect.
  - c. If the intrafraction motion is large, MLC interplay effects may be of concern (this issue is still controversial and is discussed in section 4.A.).
5. If normal tissue tolerances, based on Quantec guidelines<sup>172</sup>, relevant NRG/ RTOG protocols, or institutional criteria are exceeded, or MLC interplay effects are of concern (refer to section 4.A.), consider motion limiting techniques.
    - a. If gating, abdominal compression, respiratory limiting devices (ABC or spirometry), or tumor tracking (once developed to a clinical technique) is used, residual motion must still be included in ITV margins.
    - b. If not already planned using motion management techniques, the planning (and if necessary the planning scan) will have to be redone with the addition of such techniques.
    - c. Some centers use a motion limit (refer to section 4.A.) at the time of simulation to determine if a motion limiting technique will be used.
  6. If gating (including breath hold or treating only during certain breathing phases) is used, coaching is recommended.
    - a. Coaching improves the correlation between internal volumes and external surrogates—especially audio-video coaching.
    - b. Treatment around end expiration is more reproducible and provides longer duty cycles; although, more lung is treated than at end inspiration. If gating around end inspiration is used, video coaching or a respiratory limiting device is necessary.
    - c. Amplitude gating is somewhat more consistent and accurate than phase gating. Audio coaching alone is sufficient for phase gating, but video coaching is necessary for amplitude gating; although, this tends to be more difficult for some patients to follow<sup>87</sup>.
  7. Heterogeneity corrections are required<sup>131</sup>.
  8. Monte Carlo or convolution/superposition algorithms should be used for planning, and pencil beam algorithms should not be used<sup>131</sup>.
  9. Daily image guidance is required, and daily volumetric imaging (CBCT, 4D CBCT, or CT-on-rails) is preferred. Daily fluoroscopy is also suggested for lung SBRT patients.
  10. Respiration should be monitored throughout treatment using skin surface monitors (e.g. cameras tracking reflective markers on the torso, laser tracking systems, or strain gages), breathing monitors (e.g. spirometers or thermistors), or tracking implanted markers (e.g. fiducials or transponders). Such monitors can

be used for gating but also inform therapists of breathing irregularities including coughs, sneezes allowing them to intervene in the treatment as necessary.

Several active areas of research remain including density overrides, motion limits, optimal treatment phases, combining doses over different phases, and tumor tracking. Such research will help provide a better understanding of dose delivery and treatment response in the future. In the meantime, AAPM TG Report No. 101 has provided recommendations for performing SBRT treatments including lung and upper abdominal tumors<sup>131</sup>. This present work provides additional recommendations for performing SBRT treatments for lung and upper abdominal tumors with potential adoption in clinical trial protocols for radiotherapy guidance.

## Acknowledgments

This project was supported by NCI grants U24CA180803, U10CA180868, and PA CURE grants.

## References

1. Onishi H, Shirato H, Nagata Y, et al. Hypofractionated Stereotactic Radiotherapy (HypoFXSRT) for Stage I Non-small Cell Lung Cancer: Updated Results of 257 Patients in a Japanese Multi-institutional Study. *J Thorac Oncol.* 2007; 2(Supplement 3):S94–S100. [PubMed: 17603311]
2. Baumann P, Nyman J, Hoyer M, et al. Outcome in a prospective phase II trial of medically inoperable stage I non-small-cell lung cancer patients treated with stereotactic body radiotherapy. *J Clin Oncol.* 2009; 27(20):3290–6. [PubMed: 19414667]
3. Inoue T, Katoh N, Onimaru R, et al. Stereotactic body radiotherapy using gated radiotherapy with real-time tumor-tracking for stage I non-small cell lung cancer. *Radiat Oncol.* 2013; 8(1):69. [PubMed: 23518013]
4. Jiang SB. Technical aspects of image-guided respiration-gated radiation therapy. *Med Dosim.* 2006; 31(2):141–151. [PubMed: 16690455]
5. Fassi A, Schaerer J, Fernandes M, Riboldi M, Sarrut D, Baroni G. Tumor tracking method based on a deformable 4D CT breathing motion model driven by an external surface surrogate. *Int J Radiat Oncol Biol Phys.* 2014; 88(1):182–188. [PubMed: 24331665]
6. Shirato H, Onimaru R, Ishikawa M, et al. Real-time 4-D radiotherapy for lung cancer. *Cancer Sci.* 2012; 103(1):1–6. [PubMed: 21954991]
7. Shimizu S, Shirato H, Kagei K, et al. Impact of respiratory movement on the computed tomographic images of small lung tumors in three-dimensional (3D) radiotherapy. *Int J Radiat Oncol Biol Phys.* 2000; 46(5):1127–33. [PubMed: 10725622]
8. Shen S, Duan J, Fiveash JB, et al. Validation of target volume and position in respiratory gated CT planning and treatment. *Med Phys.* 2003; 30(12):3196–3205. [PubMed: 14713086]
9. Mageras GS, Pevsner A, Yorke ED, et al. Measurement of lung tumor motion using respiration-correlated CT. *Int J Radiat Oncol Biol Phys.* 2004; 60(3):933–941. [PubMed: 15465212]
10. Yamamoto T, Langner U, Loo BW, Shen J, Keall PJ. Retrospective Analysis of Artifacts in Four-Dimensional CT Images of 50 Abdominal and Thoracic Radiotherapy Patients. *Int J Radiat Oncol Biol Phys.* 2008; 72(4):1250–1258. [PubMed: 18823717]
11. Hugo GD, Rosu M. Advances in 4D radiation therapy for managing respiration: Part I - 4D imaging. *Z Med Phys.* 2012; 22(4):258–271. [PubMed: 22784929]
12. Benchetrit G. Breathing pattern in humans: Diversity and individuality. *Respir Physiol.* 2000; 122(2–3):123–129. [PubMed: 10967339]
13. Seppenwoolde Y, Shirato H, Kitamura K, et al. Precise and real-time measurement of 3D tumor motion in lung due to breathing and heartbeat, measured during radiotherapy. *Int J Radiat Oncol Biol Phys.* 2002; 53(4):822–834. [PubMed: 12095547]

14. McClelland JR, Hughes S, Modat M, et al. Inter-fraction variations in respiratory motion models. *Phys Med Biol*. 2011; 56(1):251–272. [PubMed: 21149951]
15. Keall PJ, Mageras GS, Balter JM, et al. The management of respiratory motion in radiation oncology report of AAPM Task Group 76. *Med Phys*. 2006; 33(10):3874–3900. [PubMed: 17089851]
16. Liu HH, Balter P, Tutt T, et al. Assessing Respiration-Induced Tumor Motion and Internal Target Volume Using Four-Dimensional Computed Tomography for Radiotherapy of Lung Cancer. *Int J Radiat Oncol Biol Phys*. 2007; 68(2):531–540. [PubMed: 17398035]
17. Hanley J, Debois MM, Mah D, et al. Deep inspiration breath-hold technique for lung tumors: The potential value of target immobilization and reduced lung density in dose escalation. *Int J Radiat Oncol Biol Phys*. 1999; 45(3):603–611. [PubMed: 10524412]
18. Balter JM, Lam KL, McGinn CJ, Lawrence TS, Ten Haken RK. Improvement of CT-based treatment-planning models of abdominal targets using static exhale imaging. *Int J Radiat Oncol*. 1998; 41(4):939–943.
19. Davies SC, Hill La, Holmes RB, Halliwell M, Jackson PC. Ultrasound quantitation of respiratory organ motion in the upper abdomen. *Br J Radiol*. 1994; 67(803):1096–102. [PubMed: 7820402]
20. Korin HW, Ehman RL, Riederer SJ, Felmlee JP, Grimm RC. Respiratory kinematics of the upper abdominal organs: a quantitative study. *Magn Reson Med*. 1992; 23(1):172–178. [PubMed: 1531152]
21. Bussels B, Goethals L, Feron M, et al. Respiration-induced movement of the upper abdominal organs: a pitfall for the three-dimensional conformal radiation treatment of pancreatic cancer. *Radiother Oncol*. 2003; 68(1):69–74. [PubMed: 12885454]
22. Shirato H, Seppenwoolde Y, Kitamura K, Onimura R, Shimizu S. Intrafractional Tumor Motion: Lung and Liver. 2004
23. Langen KM, Jones DTL. Organ motion and its management. *Int J Radiat Oncol Biol Phys*. 2001; 50(1):265–278. [PubMed: 11316572]
24. Brandner ED, Wu A, Chen H, et al. Abdominal organ motion measured using 4D CT. *Int J Radiat Oncol Biol Phys*. 2006; 65(2):554–560. [PubMed: 16690437]
25. Landberg, T., Chavaudra, J., Dobbs, H. ICRU Report 50: Prescribing, Recording, and Reporting Photon Beam Therapy. International Commission on Radiation Units and Measurements; Bethesda, Maryland; 1993.
26. Landberg, T., Chavaudra, J., Dobbs, H. ICRU Report 62: Prescribing, Recording, and Reporting Photon Beam Therapy (Supplement to ICRU Report 50). International Commission on Radiation Units and Measurements; Bethesda, Maryland; 1999.
27. Ezhil M, Vedam S, Balter P, et al. Determination of patient-specific internal gross tumor volumes for lung cancer using four-dimensional computed tomography. *Radiat Oncol*. 2009; 4:4. [PubMed: 19173738]
28. Chang JY, Dong L, Liu H, et al. Image-guided radiation therapy for non-small cell lung cancer. *J Thorac Oncol*. 2008; 3(2):177–86. [PubMed: 18303441]
29. Ekberg L, Holmberg O, Wittgren L, Bjelkengren G, Landberg T. What margins should be added to the clinical target volume in radiotherapy treatment planning for lung cancer? *Radiother Oncol*. 1998; 48(1):71–77. [PubMed: 9756174]
30. Plathow C, Ley S, Fink C, et al. Analysis of intrathoracic tumor mobility during whole breathing cycle by dynamic MRI. *Int J Radiat Oncol*. 2004; 59(4):952–959.
31. Hu Y, Caruthers SD, Low Da, Parikh PJ, Mutic S. Respiratory amplitude guided 4-dimensional magnetic resonance imaging. *Int J Radiat Oncol Biol Phys*. 2013; 86(1):198–204. [PubMed: 23414769]
32. Cai J, Chang Z, Wang Z, Paul Segars W, Yin F-F. Four-dimensional magnetic resonance imaging (4D-MRI) using image-based respiratory surrogate: A feasibility study. *Med Phys*. 2011; 38(12): 6384. [PubMed: 22149822]
33. Van Sörnsen De Koste JR, Lagerwaard FJ, Nijssen-Visser MRJ, Graveland WJ, Senan S. Tumor location cannot predict the mobility of lung tumors: A 3D analysis of data generated from multiple CT scans. *Int J Radiat Oncol Biol Phys*. 2003; 56(2):348–354. [PubMed: 12738308]

34. Rosenzweig KE, Hanley J, Mah D, et al. The deep inspiration breath-hold technique in the treatment of inoperable non-small-cell lung cancer. *Int J Radiat Oncol Biol Phys.* 2000; 48(1):81–7. [PubMed: 10924975]
35. Maxim PG, Loo BW, Shirazi H, Thorndyke B, Luxton G, Le QT. Quantification of Motion of Different Thoracic Locations Using Four-Dimensional Computed Tomography: Implications for Radiotherapy Planning. *Int J Radiat Oncol Biol Phys.* 2007; 69(5):1395–1401. [PubMed: 17869025]
36. Weiss E, Wijesooriya K, Dill SV, Keall PJ. Tumor and normal tissue motion in the thorax during respiration: Analysis of volumetric and positional variations using 4D CT. *Int J Radiat Oncol.* 2007; 67(1):296–307.
37. Sonke JJ, Lebesque J, van Herk M. Variability of Four-Dimensional Computed Tomography Patient Models. *Int J Radiat Oncol Biol Phys.* 2008; 70(2):590–598. [PubMed: 18037579]
38. Nehmeh, Sa, Erdi, YE., Pan, T., et al. Four-dimensional (4D) PET/CT imaging of the thorax. *Med Phys.* 2004; 31(2004):3179–3186. [PubMed: 15651600]
39. Nehmeh, Sa, Erdi, YE., Pan, T., et al. Quantitation of respiratory motion during 4D-PET/CT acquisition. *Med Phys.* 2004; 31(2004):1333–1338. [PubMed: 15259636]
40. Nehmeh, Sa, Erdi, YE., Ling, CC., et al. Effect of respiratory gating on reducing lung motion artifacts in PET imaging of lung cancer. *Med Phys.* 2002; 29(2002):366–371. [PubMed: 11929020]
41. Loeffler JS, Schwaab J. First steps Toward Ultrasound-Based Motion compensation for imaging and Therapy: calibration with an Optical system and 4D PeT imaging. *Front Oncol.* 2015; 5(258): 1–10. [PubMed: 25667919]
42. Schwaab J, Prall M, Sarti C, et al. *Physica Medica* Ultrasound tracking for intra-fractional motion compensation in radiation therapy. *Phys Medica.* 2014; 30(5):578–582.
43. Ekberg L, Holmberg O, Wittgren L, Bjelkengren G, Landberg T. What margins should be added to the clinical target volume in radiotherapy treatment planning for lung cancer? *Radiother Oncol.* 1998; 48:71–77. [PubMed: 9756174]
44. Brandner ED, Heron D, Wu A, Huq MS, Yue NJ, Chen H. Localizing moving targets and organs using motion-managed CTs. *Med Dosim.* 2006; 31(2):134–140. [PubMed: 16690454]
45. Keall P. 4-Dimensional Computed Tomography Imaging and Treatment Planning. *Semin Radiat Oncol.* 2004; 14(1):81–90. [PubMed: 14752736]
46. Abdelnour FA, Nehmeh Sa, Pan T, et al. Phase and amplitude binning for 4D-CT imaging. *Phys Med Biol.* 2007; 52:3515–3529. [PubMed: 17664557]
47. Hui C, Suh Y, Robertson D, et al. Internal respiratory surrogate in multislice 4D CT using a combination of Fourier transform and anatomical features. *Med Phys.* 2015; 42:4338–4348. [PubMed: 26133631]
48. Sonke J-J, Zijp L, Remeijer P, van Herk M. Respiratory correlated cone beam CT. *Med Phys.* 2005; 32(2005):1176–1186. [PubMed: 15895601]
49. Heerkens H, van Vulpen M, van den Berg C, et al. MRI-Based Tumor Motion Characterization and Gating Schemes for Radiation Therapy of Pancreatic Cancer. *Radiother Oncol.* 2014; 111(2):252–257. [PubMed: 24746577]
50. Fernandes AT, Apisarnthanarax S, Yin L, et al. Comparative Assessment of Liver Tumor Motion Using Cine-Magnetic Resonance Imaging Versus 4-Dimensional Computed Tomography. *Int J Radiat Oncol.* 2015; 91(5):1034–1040.
51. Stemkens B, Tijssen RHN, de Senneville BD, Lagendijk JJW, van den Berg CaT. Image-driven, model-based 3D abdominal motion estimation for MR-guided radiotherapy. *Phys Med Biol.* 2016; 61(14):5335–55. [PubMed: 27362636]
52. Lee D, Greer PB, Pollock S, et al. Quantifying the accuracy of the tumor motion and area as a function of acceleration factor for the simulation of the dynamic keyhole magnetic resonance imaging method Quantifying the accuracy of the tumor motion and area as a function of acceleration fact. 2016; 2639
53. Harris W, Ren L, Cai J, Zhang Y, Chang Z, Yin FF. A technique for generating volumetric cine-magnetic resonance imaging. *Int J Radiat Oncol Biol Phys.* 2016; 95(2):844–853. [PubMed: 27131085]

54. Paganelli C, Seregini M, Fattori G, et al. Magnetic resonance imaging-guided versus surrogate-based motion tracking in liver radiation therapy: A prospective comparative study. *Int J Radiat Oncol Biol Phys.* 2015; 91(4):840–848. [PubMed: 25752399]
55. van Heijst TCF, Philippens MEP, Charaghvandi RK, et al. Quantification of intra-fraction motion in breast radiotherapy using supine magnetic resonance imaging. *Phys Med Biol.* 2016; 61(3):1352–1370. [PubMed: 26797074]
56. Kleijnen JJE, van Asselen B, Burbach JPM, et al. Evolution of motion uncertainty in rectal cancer: implications for adaptive radiotherapy. *Phys Med Biol.* 2016; 61(1):1–11. [PubMed: 26605518]
57. Li H, Chen H-C, Dolly S, et al. An integrated model-driven method for in-treatment upper airway motion tracking using cine MRI in head and neck radiation therapy. *Med Phys.* 2016; 43(8):4700–4710. [PubMed: 27487887]
58. Yang YX, Teo S-K, Van Reeth E, Tan CH, Tham IWK, Poh CL. A hybrid approach for fusing 4D-MRI temporal information with 3D-CT for the study of lung and lung tumor motion. *Med Phys.* 2015; 42(8):4484–4496. [PubMed: 26233178]
59. Paganelli C, Summers P, Bellomi M, Baroni G, Riboldi M. Liver 4DMRI: A retrospective image-based sorting method. *Med Phys.* 2015; 42(8):4814–21. [PubMed: 26233208]
60. Glide-Hurst CK, Kim JP, To D, et al. Four dimensional magnetic resonance imaging optimization and implementation for magnetic resonance imaging simulation. *Pract Radiat Oncol.* 2015; 5(6):433–442. [PubMed: 26419444]
61. Tian Y, Wang Z, Ge H, et al. Dosimetric comparison of treatment plans based on free breathing, maximum, and average intensity projection CTs for lung cancer SBRT. *Med Phys.* 2012; 39(5):2754. [PubMed: 22559646]
62. Park K, Huang L, Gagne H, Papiez L. Do Maximum Intensity Projection Images Truly Capture Tumor Motion? *Int J Radiat Oncol Biol Phys.* 2009; 73(2):618–625. [PubMed: 19147026]
63. Ozhasoglu C, Murphy MJ. Issues in respiratory motion compensation during external-beam radiotherapy. *Int J Radiat Oncol Biol Phys.* 2002; 52(5):1389–1399. [PubMed: 11955754]
64. Ruan D, Fessler Ja, Balter JM, Keall PJ. Real-time profiling of respiratory motion: baseline drift, frequency variation and fundamental pattern change. *Phys Med Biol.* 2009; 54:4777–4792. [PubMed: 19622852]
65. Stock M, Kontrissova K, Dieckmann K, Bogner J, Poetter R, Georg D. Development and application of a real-time monitoring and feedback system for deep inspiration breath hold based on external marker tracking. *Med Phys.* 2006; 33(2006):2868–2877. [PubMed: 16964863]
66. George R, Chung TD, Vedam SS, et al. Audio-visual biofeedback for respiratory-gated radiotherapy: Impact of audio instruction and audio-visual biofeedback on respiratory-gated radiotherapy. *Int J Radiat Oncol Biol Phys.* 2006; 65(3):924–933. [PubMed: 16751075]
67. Stam MK, van Vulpen M, Barendrecht MM, et al. Kidney motion during free breathing and breath hold for MR-guided radiotherapy. *Phys Med Biol.* 2013; 58:2235–45. [PubMed: 23475278]
68. Siochi RA, Kim Y, Bhatia S. Tumor control probability reduction in gated radiotherapy of non-small cell lung cancers: a feasibility study. *J Appl Clin Med Phys.* 2015; 16(1):8–21. [PubMed: 28297257]
69. Wölfelschneider J, Brandt T, Lettmaier S, Fietkau R, Bert C. Quantification of an External Motion Surrogate for Quality Assurance in Lung Cancer Radiation Therapy. *Biomed Res Int.* 2014; 2014
70. Taniguchi CM, Murphy JD, Eclov N, et al. Dosimetric Analysis of Organs at Risk During Expiratory Gating in Stereotactic Body Radiation Therapy for Pancreatic Cancer. *Radiat Oncol Biol.* 2013; 85(4):1090–1095.
71. St James S, Mishra P, Hacker F, Berbeco RI, Lewis JH. Quantifying ITV instabilities arising from 4DCT: a simulation study using patient data. *Phys Med Biol.* 2012; 57:L1–L7. [PubMed: 22343122]
72. Ge J, Santanam L, Noel C, Parikh PJ. Planning 4-dimensional computed tomography (4DCT) cannot adequately represent daily intrafractional motion of abdominal tumors. *Int J Radiat Oncol Biol Phys.* 2013; 85(4):999–1005. [PubMed: 23102840]
73. Ahn S, Yi B, Suh Y, et al. A feasibility study on the prediction of tumour location in the lung from skin motion. *Br J Radiol.* 2004; 77(919):588–596. [PubMed: 15238406]

74. Bouilhol G, Ayadi M, Rit S, et al. Is abdominal compression useful in lung stereotactic body radiation therapy? A 4DCT and dosimetric lobe-dependent study. *Phys Medica*. 2013; 29(4):333–340.
75. Eccles CL, Patel R, Simeonov AK, Lockwood G, Haider M, Dawson La. Comparison of liver tumor motion with and without abdominal compression using cine-magnetic resonance imaging. *Int J Radiat Oncol Biol Phys*. 2011; 79(2):602–608. [PubMed: 20675063]
76. Heinzerling JH, Anderson JF, Papiez L, et al. Four-Dimensional Computed Tomography Scan Analysis of Tumor and Organ Motion at Varying Levels of Abdominal Compression During Stereotactic Treatment of Lung and Liver. *Int J Radiat Oncol Biol Phys*. 2008; 70(5):1571–1578. [PubMed: 18374231]
77. Mampuya WA, Matsuo Y, Ueki N, et al. The impact of abdominal compression on outcome in patients treated with stereotactic body radiotherapy for primary lung cancer. *J Radiat Res*. 2014; 55(5):934–939. [PubMed: 24801474]
78. Wunderink W, Méndez Romero A, de Kruijf W, de Boer H, Levendag P, Heijmen B. Reduction of Respiratory Liver Tumor Motion by Abdominal Compression in Stereotactic Body Frame, Analyzed by Tracking Fiducial Markers Implanted in Liver. *Int J Radiat Oncol Biol Phys*. 2008; 71(3):907–915. [PubMed: 18514783]
79. Dawson, La, Brock, KK., Kazanjian, S., et al. The reproducibility of organ position using active breathing control (ABC) during liver radiotherapy. *Int J Radiat Oncol Biol Phys*. 2001; 51(5): 1410–1421. [PubMed: 11728702]
80. Gagel B, Demirel C, Kientopf A, et al. Active breathing control (ABC): Determination and reduction of breathing-induced organ motion in the chest. *Int J Radiat Oncol Biol Phys*. 2007; 67(3):742–749. [PubMed: 17197133]
81. Wong JW, Sharpe MB, Jaffray Da, et al. The use of active breathing control (ABC) to reduce margin for breathing motion. *Int J Radiat Oncol Biol Phys*. 1999; 44(4):911–919. [PubMed: 10386650]
82. Kubo HD, Hill BC. Respiration gated radiotherapy treatment: a technical study. *Phys Med Biol*. 1996; 41:83–91. [PubMed: 8685260]
83. Murphy MJ, Martin D, Whyte R, Hai J, Ozhasoglu C, Le QT. The effectiveness of breath-holding to stabilize lung and pancreas tumors during radiosurgery. *Int J Radiat Oncol Biol Phys*. 2002; 53(2):475–482. [PubMed: 12023152]
84. Gierga DP, Brewer J, Sharp GC, Betke M, Willett CG, Chen GTY. The correlation between internal and external markers for abdominal tumors: Implications for respiratory gating. *Int J Radiat Oncol Biol Phys*. 2005; 61(5):1551–1558. [PubMed: 15817361]
85. Glide-Hurst CK, Chetty IJ. Improving radiotherapy planning, delivery accuracy, and normal tissue sparing using cutting edge technologies. *J Thorac Dis*. 2014; 6(9):303–318. [PubMed: 24688775]
86. Li G, Arora NC, Xie H, et al. Quantitative prediction of respiratory tidal volume based on the external torso volume change: a potential volumetric surrogate. *Phys Med Biol*. 2009; 54:1963–1978. [PubMed: 19265201]
87. Onishi H, Kawakami H, Marino K, et al. A simple respiratory indicator for irradiation during voluntary breath holding: a one-touch device without electronic materials. *Radiology*. 2010; 255(3):917–923. [PubMed: 20501729]
88. Shirato H, Shimizu S, Kitamura K, et al. Four-dimensional treatment planning and fluoroscopic real-time tumor tracking radiotherapy for moving tumor. *Int J Radiat Oncol Biol Phys*. 2000; 48(2):435–442. [PubMed: 10974459]
89. Vedam SS, Keall PJ, Kini VR, Mohan R. Determining parameters for respiration-gated radiotherapy. *Med Phys*. 2001; 28:2139–2146. [PubMed: 11695776]
90. Goossens S, Senny F, Lee JA, Janssens G, Geets X. Assessment of tumor motion reproducibility with audio-visual coaching through successive 4D CT sessions. *J Appl Clin Med Phys*. 2014; 15(1):47–56.
91. Nakamura M, Shibuya K, Shiinoki T, et al. Positional reproducibility of pancreatic tumors under end-exhalation breath-hold conditions using a visual feedback technique. *Int J Radiat Oncol Biol Phys*. 2011; 79(5):1565–1571. [PubMed: 20832187]



92. Burnett SSC, Sixel KE, Cheung PCF, Hoisak JDP. A study of tumor motion management in the conformal radiotherapy of lung cancer. *Radiother Oncol.* 2008; 86(1):77–85. [PubMed: 18077031]
93. Keall PJ, Mageras GS, Balter JM, et al. The management of respiratory motion in radiation oncology report of AAPM Task Group. 2006; 76
94. Hunjan S, Starkschall G, Prado K, Dong L, Balter P. Lack of Correlation Between External Fiducial Positions and Internal Tumor Positions During Breath-Hold CT. *Int J Radiat Oncol Biol Phys.* 2010; 76(5):1586–1591. [PubMed: 20133074]
95. Shirato H, Shimizu S, Kunieda T, et al. Physical aspects of a real-time tumor-tracking system for gated radiotherapy. *Int J Radiat Oncol Biol Phys.* 2000; 48(4):1187–1195. [PubMed: 11072178]
96. Falk M, Pommer T, Keall P, et al. Motion management during IMAT treatment of mobile lung tumors — A comparison of MLC tracking and gated delivery Motion management during IMAT treatment of mobile lung tumors — A comparison of MLC tracking and gated delivery. *Med Phys.* 2014; 41(10):101707. [PubMed: 25281946]
97. Tai A, Christensen JD, Gore E, Khamene A, Boettger T, Li XA. Gated Treatment Delivery Verification With On-Line Megavoltage Fluoroscopy. *Int J Radiat Oncol Biol Phys.* 2010; 76(5):1592–1598. [PubMed: 20133069]
98. Ceberg S, Falk M, Af Rosenschöld PM, et al. Tumor-tracking radiotherapy of moving targets; verification using 3D polymer gel, 2D ion-chamber array and biplanar diode array. *J Phys Conf Ser.* 2010; 250:012051.
99. Keall PJ, Sawant A, Cho B, et al. Electromagnetic-guided dynamic multileaf collimator tracking enables motion management for intensity-modulated arc therapy. *Int J Radiat Oncol Biol Phys.* 2011; 79(1):312–320. [PubMed: 20615630]
100. Keall PJ, Colvill E, O'Brien R, et al. The first clinical implementation of electromagnetic transponder-guided MLC tracking. *Med Phys.* 2014; 41(2):020702. [PubMed: 24506591]
101. Falk M, af Rosenschöld PM, Keall P, et al. Real-time dynamic MLC tracking for inversely optimized arc radiotherapy. *Radiother Oncol.* 2010; 94(2):218–223. [PubMed: 20089322]
102. Davies, Ga, Clowes, P., Bedford, JL., Evans, PM., Webb, S., Poludniowski, G. An experimental evaluation of the Agility MLC for motion-compensated VMAT delivery. *Phys Med Biol.* 2013; 58(13):4643–4657. [PubMed: 23780400]
103. Tacke MB, Nill S, Krauss A, Oelfke U. Real-time tumor tracking: Automatic compensation of target motion using the Siemens 160 MLC. *Med Phys.* 2010; 37(2):753. [PubMed: 20229885]
104. Poels K, Depuydt T, Verellen D, et al. A complementary dual-modality verification for tumor tracking on a gimbaled linac system. *Radiother Oncol.* 2013; 109(3):469–474. [PubMed: 24238982]
105. Depuydt T, Poels K, Verellen D, et al. Initial assessment of tumor tracking with a gimbaled linac system in clinical circumstances: A patient simulation study. *Radiother Oncol.* 2013; 106(2):236–240. [PubMed: 23398905]
106. Dawson, La, Sharpe, MB. Image-guided radiotherapy: rationale, benefits, and limitations. *Lancet Oncol.* 2006
107. Neicu T, Berbeco R, Wolfgang J, Jiang SB. Synchronized moving aperture radiation therapy (SMART): improvement of breathing pattern reproducibility using respiratory coaching. *Phys Med Biol.* 2006; 51:617–636. [PubMed: 16424585]
108. Kim T, Pollock S, Lee D, O'Brien R, Keall P. Audiovisual biofeedback improves diaphragm motion reproducibility in MRI. *Med Phys.* 2012; 39:6921. [PubMed: 23127085]
109. Nakamura M, Narita Y, Matsuo Y, et al. Effect of Audio Coaching on Correlation of Abdominal Displacement With Lung Tumor Motion. *Int J Radiat Oncol Biol Phys.* 2009; 75(2):558–563. [PubMed: 19735881]
110. Michalski D, Sontag M, Li F, et al. Four-Dimensional Computed Tomography-Based Interfractional Reproducibility Study of Lung Tumor Intrafractional Motion. *Int J Radiat Oncol Biol Phys.* 2008; 71(3):714–724. [PubMed: 18514778]
111. Mageras GS, Yorke E, Rosenzweig K, et al. Fluoroscopic evaluation of diaphragmatic motion reduction with a respiratory gated radiotherapy system. *J Appl Clin Med Phys.* 2001; 2(4):191–200. [PubMed: 11686740]

112. Ionascu D, Jiang SB, Nishioka S, Shirato H, Berbeco RI. Internal-external correlation investigations of respiratory induced motion of lung tumors. *Med Phys.* 2007; 34(10):3893. [PubMed: 17985635]
113. Koch N, Liu HH, Starkschall G, et al. Evaluation of internal lung motion for respiratory-gated radiotherapy using MRI: Part I - Correlating internal lung motion with skin fiducial motion. *Int J Radiat Oncol Biol Phys.* 2004; 60(5):1459–1472. [PubMed: 15590177]
114. Hoisak JDP, Sixel KE, Tirona R, Cheung PCF, Pignol JP. Correlation of lung tumor motion with external surrogate indicators of respiration. *Int J Radiat Oncol Biol Phys.* 2004; 60(4):1298–1306. [PubMed: 15519803]
115. Haasbeek, CJa, Spoelstra, FOB., Lagerwaard, FJ., et al. Impact of Audio-Coaching on the Position of Lung Tumors. *Int J Radiat Oncol Biol Phys.* 2008; 71(4):1118–1123. [PubMed: 18258386]
116. Bortfeld T, Jokivarsi K, Goitein M, Kung J, Jiang SB. Effects of intra-fraction motion on IMRT dose delivery: statistical analysis and simulation. *Phys Med Biol.* 2002; 47:2203–2220. [PubMed: 12164582]
117. Jiang SB, Pope C, Al Jarrah KM, Kung JH, Bortfeld T, Chen GTY. An experimental investigation on intra-fractional organ motion effects in lung IMRT treatments. *Phys Med Biol.* 2003; 48(12):1773–1784. [PubMed: 12870582]
118. Chen H, Wu A, Brandner ED, et al. Dosimetric evaluations of the interplay effect in respiratory-gated intensity-modulated radiation therapy. *Med Phys.* 2009; 36:893–903. [PubMed: 19378749]
119. Stambaugh C, Nelms BE, Dilling T, et al. Experimentally studied dynamic dose interplay does not meaningfully affect target dose in VMAT SBRT lung treatments. *Med Phys.* 2013; 40(2013):091710. [PubMed: 24007143]
120. Zhao B, Yang Y, Li T, Li X, Heron DE, Huq MS. Dosimetric effect of intrafraction tumor motion in phase gated lung stereotactic body radiotherapy. *Med Phys.* 2012; 39(2012):6629. [PubMed: 23127057]
121. Martel, MK. *Advances in Radiation Oncology in Lung Cancer.* Springer; Berlin: 2005.
122. Senan S, De Ruyscher D, Giraud P, Mirimanoff R, Budach V. Literature-based recommendations for treatment planning and execution in high-dose radiotherapy for lung cancer. *Radiother Oncol.* 2004; 71(2):139–46. [PubMed: 15110446]
123. Slotman BJ, Lagerwaard FJ, Senan S. 4D imaging for target definition in stereotactic radiotherapy for lung cancer. *Acta Oncol.* 2006; 45(7):966–972. [PubMed: 16982565]
124. Davis JN, Medbery C, Sharma S, Danish A, Mahadevan A. The RSSearch™ Registry: patterns of care and outcomes research on patients treated with stereotactic radiosurgery and stereotactic body radiotherapy. *Radiat Oncol.* 2013; 8:275. [PubMed: 24274599]
125. Scorsetti M, Clerici E, Comito T. Stereotactic body radiation therapy for liver metastases. *J Gastrointest Oncol.* 2014; 5:190–7. (Mi). [PubMed: 24982767]
126. Solberg TD, Balter JM, Benedict SH, et al. Quality and safety considerations in stereotactic radiosurgery and stereotactic body radiation therapy: Executive summary. *Pract Radiat Oncol.* 2012; 2:2–9. [PubMed: 25740120]
127. Van Herk M, Remeijer P, Rasch C, Lebesque VJ. The probability of correct target dosage: Dose-population histograms for deriving treatment margins in radiotherapy. *Int J Radiat Oncol Biol Phys.* 2000; 47(4):1121–1135. [PubMed: 10863086]
128. Mageras GS, Mechalakos J. Planning in the IGRT Context: Closing the Loop. *Semin Radiat Oncol.* 2007; 17(4):268–277. [PubMed: 17903704]
129. Bissonnette JP, Purdie T, Sharpe MB, et al. Image-Guided Stereotactic Lung Radiation Therapy. *Radiother Oncol.* 2005; 76(Supplement 1):S15–S16.
130. Grills IS, Hugo G, Kestin LL, et al. Image-guided radiotherapy via daily online cone-beam CT substantially reduces margin requirements for stereotactic lung radiotherapy. *Int J Radiat Oncol Biol Phys.* 2008; 70(4):1045–56. [PubMed: 18029110]
131. Benedict SH, Yenice KM, Followill D, et al. Stereotactic body radiation therapy: the report of AAPM Task Group 101. *Med Phys.* 2010; 37:4078–4101. (May). [PubMed: 20879569]

132. Sonke J-J, Rossi M, Wolthaus J, van Herk M, Damen E, Belderbos J. Frameless stereotactic body radiotherapy for lung cancer using four-dimensional cone beam CT guidance. *Int J Radiat Oncol Biol Phys.* 2009; 74(2):567–574. [PubMed: 19046825]
133. Shah C, Grills IS, Kestin LL, et al. Intrafraction variation of mean tumor position during image-guided hypofractionated stereotactic body radiotherapy for lung cancer. *Int J Radiat Oncol Biol Phys.* 2012; 82(5):1636–1641. [PubMed: 21489715]
134. Timmerman R, Abdulrahman R, Kavanagh BD, Meyer JL. Lung cancer: a model for implementing stereotactic body radiation therapy into practice. *Front Radiat Ther Oncol.* 2007; 40:368–85. [PubMed: 17641520]
135. Nagata Y, Wulf J, Lax I, et al. Stereotactic Radiotherapy of Primary Lung Cancer and Other Targets: Results of Consultant Meeting of the International Atomic Energy Agency. *Int J Radiat Oncol.* 2011; 79(3):660–669.
136. Shirato H, Shimizu S, Kitamura K, Onimaru R. Organ motion in image-guided radiotherapy: Lessons from real-time tumor-tracking radiotherapy. *Int J Clin Oncol.* 2007; 12(1):8–16. [PubMed: 17380435]
137. Zhao B, Yang Y, Li T, Li X, Heron DE, Huq MS. Statistical analysis of target motion in gated lung stereotactic body radiation therapy. *Phys Med Biol.* 2011; 56(5):1385–95. [PubMed: 21317481]
138. Nelson C, Balter P, Morice RC, et al. Evaluation of Tumor Position and PTV Margins Using Image Guidance and Respiratory Gating. *Int J Radiat Oncol Biol Phys.* 2010; 76(5):1578–1585. [PubMed: 20137865]
139. Jaffray, Da, Langen, KM., Mageras, G., et al. Safety considerations for IGRT: Executive summary. *Pract Radiat Oncol.* 2013; 3(3):167–170. [PubMed: 24175003]
140. Timmerman, RD., Michalski, J., Fowler, J., et al. RADIATION THERAPY ONCOLOGY GROUP RTOG 0236 A Phase II Trial of Stereotactic Body Radiation Therapy (SBRT) in the Treatment of Patients with Medically Inoperable Stage I/II Non-Small Cell Lung Cancer. *RTOG;* 2004.
141. Videtic, GMM., Singh, AK., Chang, JY., et al. Nrg Oncology RTOG 0915 a Randomized Phase II Study Comparing 2 Stereotactic Body Radiation Therapy (SBRT) Schedules for Medically Inoperable Patients With Stage I Peripheral Non-Small Cell Lung Cancer. *RTOG;* 2009.
142. Cardinale RM, Wu Q, Benedict SH, Kavanagh BD, Bump E, Mohan R. Determining the optimal block margin on the planning target volume for extracranial stereotactic radiotherapy. *Int J Radiat Oncol Biol Phys.* 1999; 45(2):515–520. [PubMed: 10487579]
143. Chetty IJ, Curran B, Cygler JE, et al. Report of the AAPM Task Group No. 105: Issues associated with clinical implementation of Monte Carlo-based photon and electron external beam treatment planning. *Med Phys.* 2007; 34(12):4818–4853.
144. Das IJ, Ding GX, Ahnesjö A. Small fields: Nonequilibrium radiation dosimetry. *Med Phys.* 2008; 35(1):206. [PubMed: 18293576]
145. Chetty IJ, Charland PM, Tyagi N, McShan DL, Fraass Ba, Bielajew AF. Photon beam relative dose validation of the DPM Monte Carlo code in lung-equivalent media. *Med Phys.* 2003; 30(4): 563–573. [PubMed: 12722808]
146. Jeraj R, Keall P. Monte Carlo-based inverse treatment planning. *Phys Med Biol.* 1999; 44(8): 1885–96. [PubMed: 10473202]
147. Chetty IJ, Rosu M, McShan DL, Fraass Ba, Ten Haken RK. Inverse Plan Optimization Incorporating Random Setup Uncertainties Using Monte Carlo Based Fluence Convolution. *Int J Radiat Oncol.* 2005; 63:S63.
148. McShan DL, Kessler ML, Vineberg K, Fraass Ba. Inverse plan optimization accounting for random geometric uncertainties with a multiple instance geometry approximation (MIGA). *Med Phys.* 2006; 33(5):1510–1521. [PubMed: 16752585]
149. Chetty IJ, Rosu M, McShan DL, Fraass Ba, Balter JM, Ten Haken RK. Accounting for center-of-mass target motion using convolution methods in Monte Carlo-based dose calculations of the lung. *Med Phys.* 2004; 31(4):925–932. [PubMed: 15125011]

150. Bradley JD, Nofal AN, El Naqa IM, et al. Comparison of helical, maximum intensity projection (MIP), and averaged intensity (AI) 4D CT imaging for stereotactic body radiation therapy (SBRT) planning in lung cancer. *Radiother Oncol.* 2006; 81(3):264–268. [PubMed: 17113668]
151. Lagerwaard FJ, Senan S. Lung cancer: intensity-modulated radiation therapy, four-dimensional imaging and mobility management. *Front Radiat Ther Oncol.* 2007; 40:239–52. [PubMed: 17641513]
152. Rietzel E, Liu AK, Chen GTY, Choi NC. Maximum-intensity volumes for fast contouring of lung tumors including respiratory motion in 4DCT planning. *Int J Radiat Oncol Biol Phys.* 2008; 71(4):1245–52. [PubMed: 18472367]
153. Underberg RWM, Lagerwaard FJ, Slotman BJ, Cuijpers JP, Senan S. Use of maximum intensity projections (MIP) for target volume generation in 4DCT scans for lung cancer. *Int J Radiat Oncol Biol Phys.* 2005; 63(1):253–260. [PubMed: 16111596]
154. Yakoumakis N, Winey B, Killoran J, et al. Using four-dimensional computed tomography images to optimize the internal target volume when using volume-modulated arc therapy to treat moving targets. *J Appl Clin Med Phys.* 2012; 13(6):3850. [PubMed: 23149778]
155. Yeo S-G, Kim ES. Efficient approach for determining four-dimensional computed tomography-based internal target volume in stereotactic radiotherapy of lung cancer. *Radiat Oncol J.* 2013; 31(4):247–51. [PubMed: 24501714]
156. Jin JY, Ajlouni M, Chen Q, Yin FF, Movsas B. A technique of using gated-CT images to determine internal target volume (ITV) for fractionated stereotactic lung radiotherapy. *Radiother Oncol.* 2006; 78(2):177–184. [PubMed: 16376444]
157. Tai A, Liang Z, Erickson B, Li XA. Management of respiration-induced motion with 4-dimensional computed tomography (4DCT) for pancreas irradiation. *Int J Radiat Oncol Biol Phys.* 2013; 86(5):908–913. [PubMed: 23688811]
158. Wolthaus JWH, Sonke J-J, van Herk M, et al. Comparison of Different Strategies to Use Four-Dimensional Computed Tomography in Treatment Planning for Lung Cancer Patients. *Int J Radiat Oncol.* 2008; 70(4):1229–1238.
159. Admiraal, Ma, Schuring, D., Hurkmans, CW. Dose calculations accounting for breathing motion in stereotactic lung radiotherapy based on 4D-CT and the internal target volume. *Radiother Oncol.* 2008; 86(1):55–60. [PubMed: 18082905]
160. Ehler ED, Tomé Wa. Lung 4D-IMRT treatment planning: an evaluation of three methods applied to four-dimensional data sets. *Radiother Oncol.* 2008; 88(3):319–25. [PubMed: 18703249]
161. Glide-Hurst CK, Hugo GD, Liang J, Yan D. A simplified method of four-dimensional dose accumulation using the mean patient density representation. *Med Phys.* 2008; 35(2008):5269–5277. [PubMed: 19175086]
162. Mageras GS, Yorke E. Deep Inspiration Breath Hold and Respiratory Gating Strategies for Reducing Organ Motion in Radiation Treatment. *Semin Radiat Oncol.* 2004; 14(1):65–75. [PubMed: 14752734]
163. Wiant D, Vanderstraeten C, Maurer J, Pursley J, Terrell J, Sintay BJ. On the validity of density overrides for VMAT lung SBRT planning. *Med Phys.* 2014; 41:081707. [PubMed: 25086517]
164. Mageras GS, Mechalakos J. Planning in the IGRT Context: Closing the Loop. *Semin Radiat Oncol.* 2007; 17:268–277. [PubMed: 17903704]
165. Purdie TG, Bissonnette JP, Franks K, et al. Cone-Beam Computed Tomography for On-Line Image Guidance of Lung Stereotactic Radiotherapy: Localization, Verification, and Intrafraction Tumor Position. *Int J Radiat Oncol Biol Phys.* 2007; 68(1):243–252. [PubMed: 17331671]
166. Higgins J, Bezjak A, Hope A, et al. Effect of image-guidance frequency on geometric accuracy and setup margins in radiotherapy for locally advanced lung cancer. *Int J Radiat Oncol Biol Phys.* 2011; 80(5):1330–1337. [PubMed: 20643515]
167. Hugo GD, Grills IS, Wloch J, Yan D. Intrafraction Variation in Tumor Position during Stereotactic Body Radiotherapy for Lung Cancer. *Int J Radiat Oncol.* 2008; 72(1):S610.
168. Bissonnette J-P, Balter Pa, Dong L, et al. Quality assurance for image-guided radiation therapy utilizing CT-based technologies: A report of the AAPM TG-179. *Med Phys.* 2012; 39(4):1946. [PubMed: 22482616]

169. Chang JY, Dong L, Liu H, et al. Image-Guided Radiation Therapy for Non-small Cell Lung Cancer. *J Thorac Oncol.* 2008; 3(2):177–186. [PubMed: 18303441]
170. Fan J, Lin T, Jin L, et al. MO-FG-CAMPUS-JeP3-05: Evaluation of 4D CT-On-Rails Target Localization Methods for Free Breathing Liver Stereotactic Body Radiotherapy (SBRT). *Med Phys.* 2016; 43(6):3727–3727.
171. Li XA, Liu F, Tai A, et al. Development of an online adaptive solution to account for inter- and intra-fractional variations. *Radiother Oncol.* 2011; 100(3):370–374. [PubMed: 21924781]
172. Marks LB, Ten Haken RK, Martel MK. QUANTEC. *Int J Radiat Oncol Biol Phys.* 2010; 76(3 supplement):S1–S160. [PubMed: 20171501]

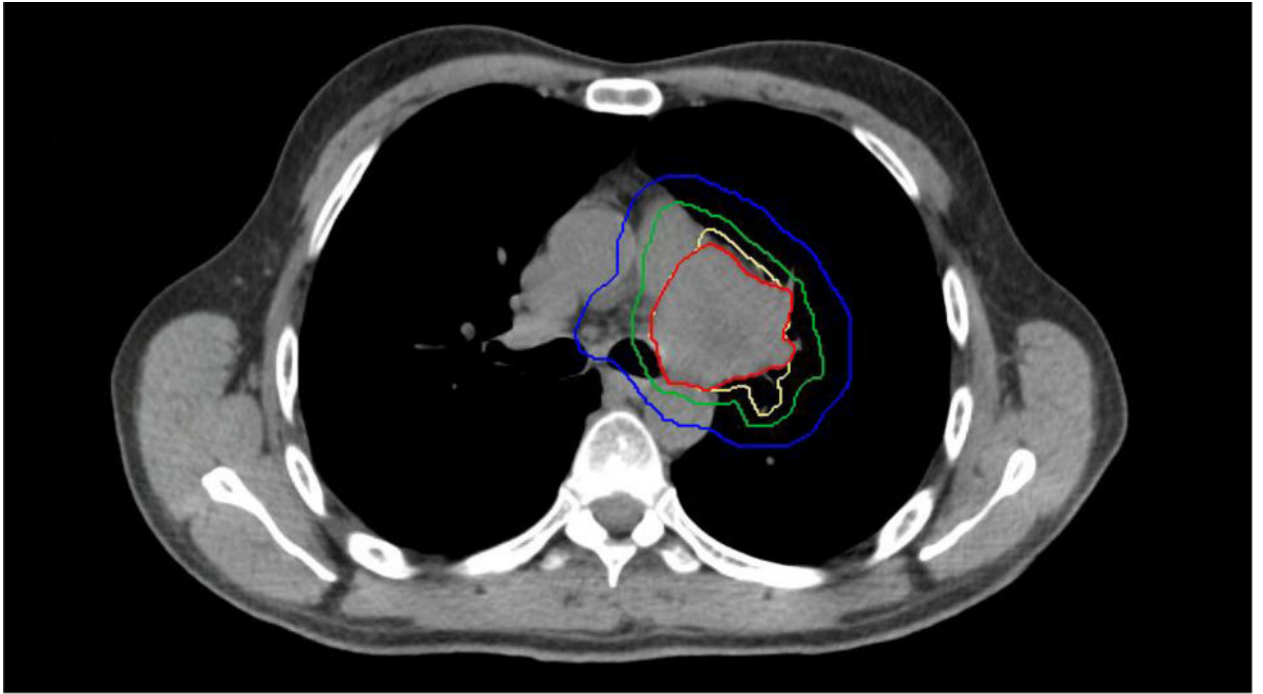


**Fig. 1.** Illustration of target volume contours: the red contour is the GTV, yellow is the IGTV, green is the ITV, and blue is the PTV.



**Table I**

## Advantages and disadvantages of various imaging modalities

Imaging Modality	Advantages	Disadvantages
Fluoroscopy	-Relatively quick. -Can evaluate motion at the time of treatment	-No cross-sectional anatomical information. -Depends on high contrast for visualization
4D CT-on-rails	-More consistent to planning CT as compared with CBCT -Accurately positions patient and localizes target for treatment -Lends itself to adaptive planning	-Requires sizably additional equipment
4D CT	-Can develop gating scheme for radiotherapy -Used for target and clinical structure delineation -Slightly better target as compared with 3D free breathing images <sup>61</sup>	-Irregular respiration adversely affects quality -Binning based on the respiratory signal can affect image quality
4D CBCT	-Powerful tool for motion evaluation on the treatment table -Accurately positions patient and localizes target for treatment -Used successfully with lung SBRT -Lends itself to adaptive planning	-Quality affected by breathing irregularities -Aliasing artifacts -Image quality is limited compared to traditional CT
4D PET/CT	-Add respiratory correlated functional imaging to a 4D CT scan -Corrects for respiratory motion artifacts in PET imaging -Improves the accuracy of the PET to CT co-registration	-Quality affected by breathing irregularities. -Aliasing artifacts -Image quality is limited compared to traditional CT
2D Cine MR imaging	-Can develop gating scheme for radiotherapy -Can detect larger differences in hepatic intra-fraction tumor motion compared with 4D CT <sup>50</sup> -No ionizing radiation -Excellent soft tissue delineation -can facilitate the development of motion models <sup>51</sup> -Can observe respiratory motion for extended lengths of time	No volumetric information
4D MR imaging	-Can develop a gating scheme for radiotherapy -Excellent soft tissue delineation -Powerful method for observing internal organ motion -Does not use ionizing radiation	-Binning based on the respiratory signal can affect the quality -MR planning not yet developed
4D Ultrasound	-Does not use ionizing radiation	-Not developed for 4D abdominal imaging